SSSTJ
Vol. 3 No.1
January 2016
ISSN 2351-0889

Suan Sunandha Science and Technology Journal

SSST JOURNAL of Science and Technology

Faculty of Science and Technology,
Suan Sunandha Rajabhat University

Available online at www.ssstj.sci.ssru.ac.th

Suan Sunandha Science and Technology Journal

General Information

The Suan Sunandha Science and Technology Journal (SSSTJ) is a double-blind peer reviewed scientific journal published twice a year (January and July) by the Faculty of Science and Technology, Suan Sunandha Rajabhat University. Submissions of manuscripts should be sent to the Editor of the SSSTJ by online system: http://www.ssstj.sci.ssru.ac.th. The manuscript will be taken that all contributing authors attest that manuscripts and material submitted to the SSSTJ are original and have not been published or submitted elsewhere and the authors concede to the open-access distribution of the manuscript, including all content contained therein.

Aim and scope:
Suan Sunandha Science and Technology Journal (SSSTJ) is an international academic journal that gains foothold at Suan Sunandha Rajabhat University, Thailand and opens to scientific communications in Southeast Asia, Asia and worldwide. It aims to contribute significant articles in science and technology researches. Published papers are focus on state of the art science and technology. Committee of the journal and association will review submitted papers. The authors may include researchers, managers, operators, students, teachers and developers.

Following areas are considered for publication:
1. Applied Physics
2. Applied Statistics
3. Biology
4. Biotechnology
5. Chemistry
6. Computer Science
7. Energy
8. Environmental Science and Technology
9. Information Technology
10. Mathematics
11. Microbiology
12. Food Science and Technology
13. Forensic Science
14. Sport Science
15. Other related fields

Available online at www.ssstj.sci.ssru.ac.th

Suan Sunandha Science and Technology Journal

Suan Sunandha Science and Technology Journal

SSSTJ Authors Guide

Types of paper:

Full length articles are typically 4 - 10 manuscript pages (including tables, figures, equations and formulas). The articles may cover a variety of topics which are related to science or technology. Articles must use previously published works to support the discussion of a particular subject or topic**.**

Plagiarism:

Submission of an manuscript implies that the work described has not been published previously (except in the form of an abstract or as part of a published lecture or academic thesis), that it is not under consideration for publication elsewhere, that its publication is approved by all authors and tacitly or explicitly by the responsible authorities where the work was carried out, and that, if accepted, it will not be published elsewhere in the same form, in English or in any other language, without the written consent of the copyright-holder.
Articles and any other material published in the SSSTJ the opinions of the author(s) and should not be construed to reflect the opinions of the editor(s) or the publisher. Manuscripts that do not meet the general criteria or standards for publication in the SSSTJ will be immediately returned to the authors, without detailed review. At their discretion, editors may request from the corresponding author a statement describing specific original contributions made by each co-author.

Manuscript submission:

For submission of all manuscripts, follow the instructions of the online submission system. Hard copy submissions cannot be accepted. Before submission, prepare and keep ready all information on the manuscript (title, full name and affiliation of all authors, corresponding author email, abstract, name of all files to be submitted).The author submitting the manuscript will be corresponding author. Manuscripts are accepted only in American English. All submitted articles should report original, previously unpublished research results, experimental or theoretical, and will be peer-reviewed.

Suan Sunandha Science and Technology Journal

Role of the funding agency:
You are requested to identify who provided financial support for conducting the research and/or preparation of the article and to briefly describe the role of the sponsor(s), if any, in study design; in the collection, analysis and interpretation of data; in the writing of the report; and in the decision to submit the article for publication. If the funding source(s) had no such involvement then this should be stated.

Journal access:

Open access:
• Articles are freely available to both subscribers and the wider public
• Articles are made available to subscribers at http://www.ssstj.sci.ssru.ac.th
Regardless of how you choose to publish your article, the journal will apply the same peer review criteria and acceptance standards.

Peer review:
All published journal papers are refereed by the international competent researchers and scientists. Therefore, a full double - blind international refereeing process is used in which 1) Papers are sent to reviewers for their peer review process. 2) The reviewers' recommendations determine whether a paper will be accepted / accepted subject to change / subject to resubmission with significant changes / rejected. For papers which require changes, the same reviewers will be used to ensure that the quality of the revised paper is acceptable. All papers are refereed, and the Editor-in-Chief reserves the right to refuse any typescript, whether on invitation or otherwise, and to make suggestions and/or modifications before publication.

Additional information:
Manuscripts must be submitted by the senior author, who must accept responsibility on behalf of all authors for all ethical requirements. The author submitting the manuscript will be listed as the corresponding author in the published version of each accepted manuscript. There are no submission fees or page charges.
Revised manuscripts should be returned including revision notes. The revision notes should address the issues raised in the referee report and clearly state per page (indicate paragraph and line) which changes have been made. Additional materials may be requested at the discretion of the editor. Authors requested to revise their submission to SSSTJ will be given 4 weeks in which to submit the revised submission. Revised submissions received after 4 weeks from the time at which the revision was requested will be considered as new submissions.

References:
There are no strict requirements on reference formatting at submission. But the authors are expected to follow the American Psychological Association (APA 6^{th} edition) style. Where applicable, author(s) name(s), journal title/book title, chapter title/article title, year of publication, volume number/book chapter and the pagination must be present. Use of DOI is highly encouraged.

Article structure:
Subdivision - numbered sections
Divide your article into clearly defined and numbered sections. Subsections should be numbered 1.1, 1.2, etc. (the abstract is not included in section numbering). Use this numbering also for internal cross-

Suan Sunandha Science and Technology Journal

referencing: do not just refer to 'the text'. Any subsection may be given a brief heading. Each heading should appear on its own separate line.

Article formatting:

Full-length articles published in the SSSTJ should include a title, the author's name, the author's address, corresponding author email, Abstract, Introduction, Materials and Methods, Results and Discussion, Acknowledgements, References.

- **Font:** Times New Roman (headings 11pt and normal text 10pt)
- **Title:** Concise and informative. This should briefly summarize the scope of the article. Avoid abbreviations and formulas where possible. The title should be centered at the top of the page. e.g., Notes on the Biology of *Varanus semiremix*
- **Authors name and affiliation:** The full names referenced by numerical superscripts with affiliation and addresses of all authors, and the full address of the corresponding author. The name of the corresponding author along with phone, fax and E-mail information. e.g.

  Author's Name
  Author's affiliation
  Author's address
  Corresponding author email
- **Corresponding author:** Clearly indicate who will handle correspondence at all stages of refereeing and publication, also post-publication. Ensure that the e-mail address is given and that contact details are kept up to date by the corresponding author.
- **Abstract:** The abstract should contain brief information on purpose, methods, results and conclusion (without subheadings). It indicates significant data, and point out major findings and conclusions. Provide 200 – 250 words in length.
- **Keywords:** 3 – 6 keywords should be listed.
- **Introduction**: The introduction should provide sufficient background knowledge and information to allow the reader to understand and evaluate the value of the study. It must also supply a rationale for the study. Cite references to provide the most salient background rather than an exhaustive review of the topic.
- **Materials and Methods:** Specific details about materials, instrumentation and experimental protocols should be given here. This section should contain sufficient details so that others are able to reproduce the experiment(s). The source of special equipment or chemicals should also be given with the name and location of manufacturers, e.g. (Merck, Germany) or (Sigma, USA). Techniques previously published or standardized can be simplified by literature citations. The statistical procedures used should be explained. Primary headings for this section are in bold, indented, with numbering. The text is run from a new line under the heading with an indentation.
- **Results and Discussions:** The results should be presented with clarity and precision. The discussions should provide an interpretation of the data and relate them to existing knowledge. Emphasis should be given to important new findings and new hypotheses should be described clearly. This section may be subdivided and headed as in the Materials and Methods section. At the end of this section, the authors should state the conclusion in a few sentences.
- **Conclusion:** The main conclusions of the study may be presented in a short Conclusions section, which may stand alone or form a subsection of a Results and Discussions section.
- **Acknowledgment:** The acknowledgments should be stated in separate section at the end of the article before the references.
- **References:** Please make sure that every reference cited in the text is also present in the reference list and vice versa.

- **Appendices (optional):** If there is more than one appendix, they should be identified as A, B, etc. Formulae and equations in appendices should be given separate numbering: Eq. (A.1), Eq. (A.2), etc.; in a subsequent appendix, Eq. (B.1) and so on. Similarly for tables and figures: Table A.1; Figure. A.1, etc.

- **Table and Figures:**
  Table: Please submit tables as editable text and not as image. Tables must be embedded in to text. Headings should be in bold letters, and aligned in the text left. Vertical lines are not used. A table should not exceed one page when printed. Use lower case letters in superscripts a, b, c ... for special remarks.
  Figure legends: It should be typed in numerical order. Begin each legend with a title and include sufficient description so that the figure is understandable without reading the text of the manuscript.
  Figures: Each figure must be embedded in to text. It should be prepared using applications capable of generating high resolution TIFF, JPEG, PNG.
  • Color or grayscale photographs: minimum of 300 dpi
  • Bitmapped line drawings: minimum of 1000 dpi
  • Combination bitmapped line (color or grayscale photographs: minimum of 500 dpi)
  • Headings should be in bold letters, and aligned in the text Centre

Checklist before submission:
The following list will be useful during the final checking of an article prior to sending it to the journal for review.
Ensure that the following contents are present:
One author has been designated as the corresponding author with contact details:
• E-mail address
• Affiliation
• Full postal address
• Corresponding author email
All necessary files have been uploaded, and contain:
• Keywords
• All figure captions
• All tables (including title, description)
• Manuscript has been 'spell-checked' (Spellchecker tool of MS word) and 'grammar-checked'
• All references mentioned in the reference list are cited in the text, and vice versa
Additional Information: For additional information regarding format, content, submissions, or authoring guidelines, please contact the editor (Email: ssstj.contact@gmail.com).

Proofs:
Proofs will be sent to the author and should be promptly returned to the editor. A total of 500 copies of each issue of the journal will be printed. Authors will receive pdf files of their article.

Biannual
ISSN 2351-0889
Subject: Science and Technology
Published by: Faculty of Science and Technology, Suan Sunandha Rajabhat University

SUAN SUNANDHA SCIENCE AND TECHNOLOGY JOURNAL

Suan Sunandha Rajabhat University, Faculty of Science and Technology
1 U-thong Nok Road, Dusit, Bangkok 10300 THAILAND

CONTENTS

Volume 3, No.1 **January 2016**

Available online at http://www.ssstj.sci.ssru.ac.th

Suan Sunandha Science and Technology Journal

An Extended Mixture Inverse Gaussian Distribution

Chookait Pudprommarat*

Faculty of Science and Technology, Suan Sunandha Rajabhat University
U-thong Nok Road, Dusit, Bangkok 10300, Thailand

Corresponding author E-mail: *chookait.pu@ssru.ac.th

Abstract: This paper proposes an extend mixture inverse Gaussian (EMIG) distribution which is mixed between the inverse Gaussian distribution and the length biased inverse Gaussian (LBIG) distribution. The Birnbaum-Saunders (BS) distribution and LBIG distribution are presented as special cases of the EMIG distribution. The properties of this distribution are discussed which include the shapes of the probability density functions, distribution functions survival functions and hazard rate functions, mean and variance. The EMIG has two parameters and it is shown that maximum likelihood estimation (MLE) can be obtained by solving equation. An application of the model to a real data set is analyzed using the new distribution, which shows that the EMIG distribution can be used quite effectively in analyzing real data by using Akaike's information criterion (AIC) statistics and goodness of fit tests.

Keywords: Mixture inverse Gaussian distribution, Length biased inverse Gaussian distribution, Birnbaum-Saunders distribution

1. Introduction

The inverse Gaussian (IG) distribution is a continuous non-negative random variable which is a right skewed distribution and it plays an important role in reliability analysis. Jorgensen et al. (1991), Gupta and Akman (1995), and Henze et al. (2002) studied the IG distribution.

Let $X_1 \sim \text{IG}(a,b)$, i.e. X_1 has a IG distribution with the parameters $a > 0$, $b > 0$ and its probability density function (pdf) and distribution function are given by

$$f_{X_1}(x_1;a,b)=\frac{a}{b\sqrt{2\pi}}\left(\frac{a}{x_1}\right)^{3/2}\exp\left[-\frac{1}{2}\left(\sqrt{\frac{x_1}{b}}-a\sqrt{\frac{b}{x_1}}\right)^2\right],$$

$$F_{X_1}(x_1;a,b)=\Phi\left(\sqrt{\frac{x_1}{b}}-a\sqrt{\frac{b}{x_1}}\right)+\Phi\left(-\left(\sqrt{\frac{x_1}{b}}+a\sqrt{\frac{b}{x_1}}\right)\right)\exp(2a),$$

where Φ (.) is the distribution function of the standard normal distribution.

The length biased inverse Gaussian (LBIG) distribution is a weighted distribution by mean of IG distribution which has received considerable attention due to its various applications in different biomedical areas, such as family history of diseases, early detection of diseases, latency periods of AIDS etc. (Akman and Gupta, 1992; Gupta and Akman,1995). The LBIG distribution was studied by Jorgensen et al. (1991), Akman and Gupta (1992) and Gupta and Akman (1995).

Let $X_2 \sim \text{LBIG}(a,b)$, then X_2 has a LBIG distribution with the parameters $a > 0$, $b > 0$ and its pdf and distribution function are given as follows

$$f_{X_2}(x_2;a,b)=\frac{1}{b\sqrt{2\pi}}\left(\frac{b}{x_2}\right)^{1/2}\exp\left[-\frac{1}{2}\left(\sqrt{\frac{x_2}{b}}-a\sqrt{\frac{b}{x_2}}\right)^2\right],$$

$$F_{X_2}(x_2;a,b)=\Phi\left(\sqrt{\frac{x_2}{b}}-a\sqrt{\frac{b}{x_2}}\right)-\exp(2a)\Phi\left(-\left(\sqrt{\frac{x_2}{b}}+a\sqrt{\frac{b}{x_2}}\right)\right).$$

The mixture inverse Gaussian (MIG) distribution, also known as the weighted inverse Gaussian distribution or the three-parameters generalized inverse Gaussian distribution or, which is mixed between the IG distribution and the LBIG distribution which was studied by Jorgensen et al. (1991), and Gupta and Akman, (1995).

Let $X \sim \text{MIG}(a,b,p)$, then X has a MIG distribution with the parameters $a > 0$, $b > 0$ and $0 \le p \le 1$, which pdf is given by

$$f_X(x;a,b,p)=pf_{X_1}(x;a,b)+(1-p)f_{X_2}(x;a,b),$$

where X_1 is random variable of IG distribution and X_2 is random variable of LBIG distribution

Then, the pdf of MIG can be written in the form:

$$f_X(x)=\frac{1}{b\sqrt{2\pi}}\left[pa\left(\frac{b}{x}\right)^{3/2}+(1-p)\left(\frac{b}{x}\right)^{1/2}\right]$$

$$f_X(x)=\frac{1}{b\sqrt{2\pi}}\left[pa\left(\frac{b}{x}\right)^{3/2}+(1-p)\left(\frac{b}{x}\right)^{1/2}\right]$$

$$\times\exp\left[-\frac{1}{2}\left(\sqrt{\frac{x}{b}}-a\sqrt{\frac{b}{x}}\right)^2\right],\quad x>0,$$

Suan Sunandha Science and Technology Journal

where $a > 0$, $b > 0$ and $0 \le p \le 1$.

For MIG distribution has several interesting special cases. In particular, the MIG (a,b,p) distribution becomes the LBIG distribution when $p=0$, the IG distribution when $p=1$ and Birnbaum-Saunders (BS) distribution (Gupta, 2011) when $p=0.5$. Although, the MIG distribution has many desirable properties in applications, parameter estimation may still have problems which have mentioned that finding the efficient initial guesses and solving the non-linear equations simultaneously are non-trivial issues (Jorgensen et al.,1991; Gupta and Akman,1995). Therefore, in order to solve such problems, a new weight parameter p is considered. We propose an extended mixture inverse Gaussian distribution which is obtained by adding a new weight parameter p to the mixture inverse Gaussian distribution.

In this paper, we present an extended mixture inverse Gaussian (EMIG) distribution. Several properties of the new distribution including the probability density functions, distribution functions, survival functions, hazard rate functions, cumulants and moments are provided. In addition, we use maximum likelihood estimation for parameter estimation and present the comparison analysis between the extended mixture inverse Gaussian distributions based on a real data set using Akaike's Information Criterion (AIC) statistics and goodness of fit tests.

2. Material and Methods

In this part, we introduce the definition of the an extended mixture inverse Gaussian distribution denoted by $X \sim \text{EMIG}(a,b)$. We begin with a general definition of the EMIG distribution which will consequently reveal its probability density function.

Definition 1. Let X_1 and X_2 be independent random variables such that $X_1 \sim \text{IG}(a,b)$ and $X_2 \sim \text{LBIG}(a,b)$. Then the new random variable X is said to have an EMIG distribution with parameter $a > 0$ and $b > 0$ if the pdf of X is defined by

$$f_X(x;a,b) = \left(\frac{a}{a+1}\right) f_{X_1}(x;a,b) + \left(\frac{1}{a+1}\right) f_{X_2}(x;a,b).$$

Theorem 1. Let X be a random variable of the EMIG distribution with parameters a and b. The pdf of X is given by

$$f(x) = \frac{1}{(a+1)b\sqrt{2\pi}}\left[a^2\left(\frac{b}{x}\right)^{3/2} + \left(\frac{b}{x}\right)^{1/2}\right] \times \exp\left[-\frac{1}{2}\left(\sqrt{\frac{x}{b}} - a\sqrt{\frac{b}{x}}\right)^2\right], \quad x > 0$$

where $a > 0$ and $b > 0$.

Proof: From Definition 1, the pdf of the EMIG distribution can be obtained by

$$\begin{aligned} f(x) &= \left(\frac{a}{a+1}\right)\frac{a}{b\sqrt{2\pi}}\left(\frac{b}{x}\right)^{3/2}\exp\left[-\frac{1}{2}\left(\sqrt{\frac{x}{b}} - a\sqrt{\frac{b}{x}}\right)^2\right] \\ &\quad + \left(\frac{1}{a+1}\right)\frac{1}{b\sqrt{2\pi}}\left(\frac{b}{x}\right)^{1/2}\exp\left[-\frac{1}{2}\left(\sqrt{\frac{x}{b}} - a\sqrt{\frac{b}{x}}\right)^2\right] \\ &= \frac{1}{(a+1)b\sqrt{2\pi}}\left[a^2\left(\frac{b}{x}\right)^{3/2} + \left(\frac{b}{x}\right)^{1/2}\right]\exp\left[-\frac{1}{2}\left(\sqrt{\frac{x}{b}} - a\sqrt{\frac{b}{x}}\right)^2\right]. \end{aligned}$$

Corollary 1. If $a=0$ then EMIG distribution reduces to LBIG distribution with parameter $a = 0$ and $b > 0$ with pdf given by

$$f(x) = \frac{1}{b\sqrt{2\pi}}\left[\left(\frac{b}{x}\right)^{1/2}\right]\exp\left[-\frac{1}{2}\left(\sqrt{\frac{x}{b}}\right)^2\right]$$

Corollary 2. If $a=1$ then EMIG distribution reduces to BS distribution with parameter $a = 1$ and $b > 0$ with pdf given by

$$f(x) = \frac{1}{2b\sqrt{2\pi}}\left[\left(\frac{b}{x}\right)^{3/2} + \left(\frac{b}{x}\right)^{1/2}\right]\exp\left[-\frac{1}{2}\left(\sqrt{\frac{x}{b}} - \sqrt{\frac{b}{x}}\right)^2\right]$$

Some parameters of the EMIG distribution and their probability density functions are provided in Figure 1.

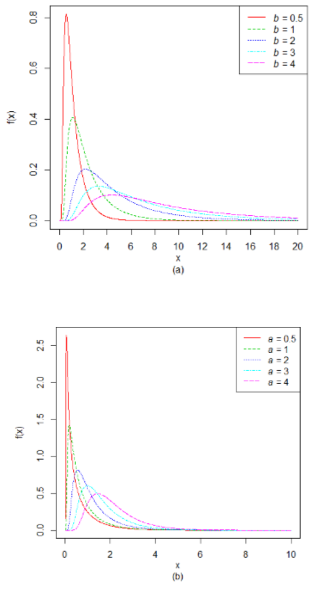

Figure 1. The probability density functions of the EMIG distribution for some values of parameters (a) $a=2$ and (b) $b=0.5$.

Suan Sunandha Science and Technology Journal

Theorem 2. Let X be a random variable of the EMIG distribution with parameters a and b. The distribution function of X is given by

$$F(x)=\Phi\left(\sqrt{\frac{x}{b}}-a\sqrt{\frac{b}{x}}\right)-\left\{\frac{1-a}{a+1}\times\exp(2a)\left[1-\Phi\left(\sqrt{\frac{x}{b}}+a\sqrt{\frac{b}{x}}\right)\right]\right\}, x>0$$

where Φ (.) is the distribution function of the standard normal distribution.

Proof: Let X is a continuous non-negative random variable, then the distribution function of X is given by

$$F(x)=\int_0^x f(t)\,dt.$$

If the distribution function of X is EMIG distribution, which is expressed by

$$F(x)=\frac{a}{a+1}\int_0^x\frac{a}{b\sqrt{2\pi}}\left(\frac{b}{t}\right)^{3/2}\exp\left[-\frac{1}{2}\left(\sqrt{\frac{t}{b}}-a\sqrt{\frac{b}{t}}\right)^2\right]dt$$
$$+\frac{1}{a+1}\int_0^x\frac{1}{b\sqrt{2\pi}}\left(\frac{b}{t}\right)^{1/2}\exp\left[-\frac{1}{2}\left(\sqrt{\frac{t}{b}}-a\sqrt{\frac{b}{t}}\right)^2\right]dt.$$

Using the distribution function of IG and LBIG distributions, then distribution function of EMIG becomes

$$F(x)=\frac{a}{a+1}\left[\Phi\left(\sqrt{\frac{x}{b}}-a\sqrt{\frac{b}{x}}\right)+\Phi\left(-\left(\sqrt{\frac{x}{b}}+a\sqrt{\frac{b}{x}}\right)\right)\exp(2a)\right]$$
$$+\frac{1}{a+1}\left[\Phi\left(\sqrt{\frac{x}{b}}-a\sqrt{\frac{b}{x}}\right)-\exp(2a)\Phi\left(-\left(\sqrt{\frac{x}{b}}+a\sqrt{\frac{b}{x}}\right)\right)\right]$$
$$=\Phi\left(\sqrt{\frac{x}{b}}-a\sqrt{\frac{b}{x}}\right)-\frac{1-a}{a+1}\exp(2a)\left[1-\Phi\left(\sqrt{\frac{x}{b}}+a\sqrt{\frac{b}{x}}\right)\right]$$

The distribution functions of the EMIG with some parameter values are shown in Figure 2.

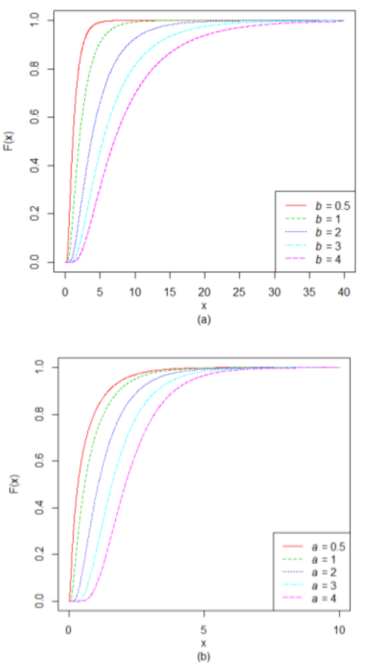

Figure 2. Distribution functions of EMIG for some values of parameters: (a) $a=2$ and (b) $b=0.5$.

Theorem 3. Let X be a random variable of the EMIG distribution with parameters a and b. The survival function of X is given by

$$S(x)=1-\Phi\left(\sqrt{\frac{x}{b}}-a\sqrt{\frac{b}{x}}\right)+\left\{\frac{1-a}{a+1}\times\exp(2a)\left[1-\Phi\left(\sqrt{\frac{x}{b}}+a\sqrt{\frac{b}{x}}\right)\right]\right\}.$$

Proof: Let X is a continuous random variable with distribution function $F(x)$ on the interval $[0,\infty)$ then the survival function is defined by $S(x)=\int_x^\infty f(t)\,dt=1-F(x)$. From the distribution function of EMIG in Theorem 2, then the survival function of X is given by

$$S(x)=1-\left\{\Phi\left(\sqrt{\frac{x}{b}}-a\sqrt{\frac{b}{x}}\right)-\frac{1-a}{a+1}\exp(2a)\left[1-\Phi\left(\sqrt{\frac{x}{b}}+a\sqrt{\frac{b}{x}}\right)\right]\right\}$$
$$=1-\Phi\left(\sqrt{\frac{x}{b}}-a\sqrt{\frac{b}{x}}\right)+\frac{1-a}{a+1}\exp(2a)\left[1-\Phi\left(\sqrt{\frac{x}{b}}+a\sqrt{\frac{b}{x}}\right)\right].$$

Theorem 4. Let X be a random variable of the EMIG distribution with parameters a and b. The hazard rate function of X can be written as

Suan Sunandha Science and Technology Journal

$$h(x)=\frac{\frac{1}{(a+1)b\sqrt{2\pi}}\left[a^2\left(\frac{b}{x}\right)^{3/2}+\left(\frac{b}{x}\right)^{1/2}\right]\exp\left[-\frac{1}{2}\left(\sqrt{\frac{x}{b}}-a\sqrt{\frac{b}{x}}\right)^2\right]}{1-\Phi\left(\sqrt{\frac{x}{b}}-a\sqrt{\frac{b}{x}}\right)+\frac{1-a}{a+1}\exp(2a)\left[1-\Phi\left(\sqrt{\frac{x}{b}}+a\sqrt{\frac{b}{x}}\right)\right]}.$$

Proof: Let X is an continuous non-negative random variable with the probability density function and survival function then the hazard rate function can be defined as

$$h(x)=\frac{f(x)}{S(x)},$$

By using $f(x)$ in Theorem 1 and $S(x)$ in Theorem 3, we have

$$h(x)=\frac{\frac{1}{b(a+1)\sqrt{2\pi}}\left[a^2 b\left(\frac{b}{x}\right)^{3/2}+\left(\frac{b}{x}\right)^{1/2}\right]\exp\left[-\frac{1}{2}\left(\sqrt{\frac{x}{b}}-a\sqrt{\frac{b}{x}}\right)^2\right]}{1-\Phi\left(\sqrt{\frac{x}{b}}-a\sqrt{\frac{b}{x}}\right)+\frac{1-a}{a+1}\exp(2a)\left[1-\Phi\left(\sqrt{\frac{x}{b}}+a\sqrt{\frac{b}{x}}\right)\right]}.$$

Some Survival functions and hazard rate functions plots of the EMIG distribution with some parameter values are displayed in Figure 3 and Figure 4

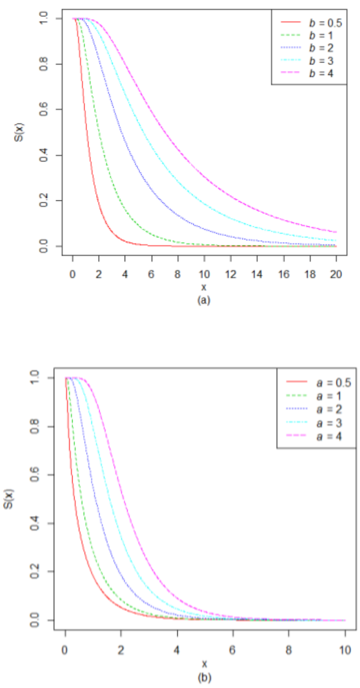

Figure 3. Survival functions of the EMIG distribution for some values of parameters: (a) $a=2$ and (b) $b=0.5$.

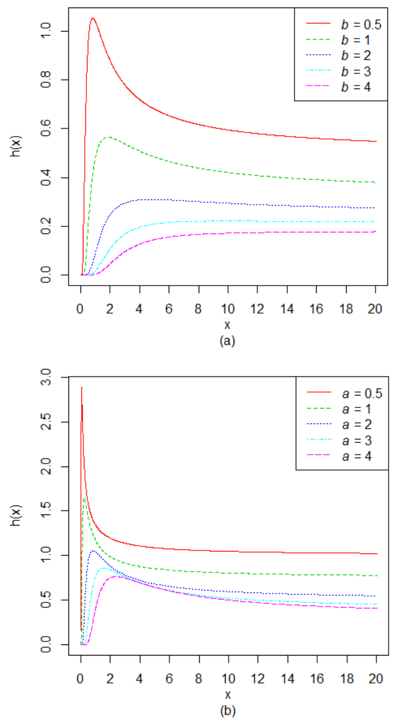

Figure 4. Hazard rate functions of the EMIG distribution for some values of parameters: (a) $a=2$ and (b) $b=0.5$.

3. Results
3.1 Theoretical results
3.1.1 Statistical Properties of the EMIG

The characteristic function, cumulants, moments, mean and variance of EMIG distribution are studied in this section.

Theorem 5. Let X be a random variable of the EMIG distribution with parameters a and b. The characteristic function of X can be written in the form

$$\varphi_X(t)=\frac{\exp\left[a\left(1-\sqrt{1-2bti}\right)\right]}{\sqrt{1-2bti}}\left(\frac{1+a\sqrt{1-2bti}}{a+1}\right).$$

Proof: The characteristic function of a random variable X is defined by

$$\varphi_X(t)=E\left(e^{itx}\right).$$

The distribution of X is a EMIG distribution, the characteristic function takes the form

$$\varphi_X(t)=\int_0^\infty \exp(itx)\frac{1}{(a+1)b\sqrt{2\pi}}\left[a^2\left(\frac{b}{x}\right)^{3/2}+\left(\frac{b}{x}\right)^{1/2}\right]$$
$$\times\exp\left[-\frac{1}{2}\left(\sqrt{\frac{x}{b}}-a\sqrt{\frac{b}{x}}\right)^2\right]dx$$

Suan Sunandha Science and Technology Journal

$$=\frac{1}{(a+1)b\sqrt{2\pi}}\int_0^\infty a^2\left(\frac{b}{x}\right)^{3/2}\exp\left[itx-\frac{1}{2}\left(\frac{x}{b}-2a+\frac{a^2b}{x}\right)\right]dx$$

$$+\frac{1}{(a+1)b\sqrt{2\pi}}\int_0^\infty \left(\frac{b}{x}\right)^{1/2}\exp\left[itx-\frac{1}{2}\left(\frac{x}{b}-2a+\frac{a^2b}{x}\right)\right]dx$$

$$=\frac{a^2b^{1/2}\exp(a)}{(a+1)\sqrt{2\pi}}\int_0^\infty x^{-3/2}\exp\left[-\left(\frac{1}{2b}-ti\right)x-\frac{a^2b/2}{x}\right]dx$$

$$+\frac{\exp(a)}{\sqrt{b}(a+1)\sqrt{2\pi}}\int_0^\infty x^{-1/2}\exp\left[-\left(\frac{1}{2b}-ti\right)x-\frac{a^2b/2}{x}\right]dx.$$

From the Table of integrals, series, and products by Gradshteyn and Ryzhik 2007, pp.369), the formulas are taken from the following form:

$$\int_0^\infty x^{-n-1/2}\exp(-\rho x-q/x)dx=(-1)^n\sqrt{\frac{\pi}{\rho}}\frac{\partial^n}{\partial q^n}\exp\left(-2\sqrt{\rho q}\right),$$

where $\operatorname{Re}\rho>0, \operatorname{Re}q>0.$

The characteristic function can become

$$\varphi_X(t)=\frac{a^2b^{1/2}\exp(a)}{(a+1)\sqrt{2\pi}}\sqrt{\frac{2\pi}{a^2b}}\exp\left(-a\sqrt{1-2bti}\right)$$

$$+\frac{\exp(a)}{\sqrt{b}(a+1)\sqrt{2\pi}}\sqrt{\frac{2b\pi}{1-2bti}}\exp\left(-a\sqrt{1-2bti}\right)$$

$$=\frac{\exp\left[a\left(1-\sqrt{1-2bti}\right)\right]}{\sqrt{1-2bti}}\left(\frac{1+a\sqrt{1-2bti}}{a+1}\right).$$

Theorem 6. Let X be a random variable of the EMIG distribution with parameters a and b. The cumulant generating function of X can be given by

$$K_X(t)=\log\left\{\left[\frac{a}{a+1}+\frac{(1-2bti)^{-1/2}}{a+1}\right]\exp\left[a\left(1-(1-2bti)^{1/2}\right)\right]\right\}.$$

Proof: The cumulant generating function of a random variable X is defined as

$$K_X(t)=\log\varphi_X(t)$$

$$K_X(t)=\log\left\{\frac{\exp\left[a\left(1-\sqrt{1-2bti}\right)\right]}{\sqrt{1-2bti}}\left(\frac{1+a\sqrt{1-2bti}}{a+1}\right)\right\}$$

$$=\log\left\{\left[\frac{1+a\sqrt{1-2bti}}{(a+1)\sqrt{1-2bti}}\right]\exp\left[a\left(1-\sqrt{1-2bti}\right)\right]\right\}$$

$$=\log\left\{\left[\frac{a}{a+1}+\frac{(1-2bti)^{-1/2}}{a+1}\right]\exp\left[a\left(1-\sqrt{1-2bti}\right)\right]\right\}.$$

Recall that a Maclaurin series, is defined as $\sum_{n=0}^{\infty}\frac{f^{(n)}}{n!}x^n.$ For $n=4,$ we have

$$f(x)=f(0)+\frac{f^{(1)}(0)}{1!}x+\frac{f^{(2)}(0)}{2!}x^2+\frac{f^{(3)}(0)}{3!}x^3+\frac{f^{(4)}(0)}{4!}x^4+O\left(x^5\right).$$

Thus, the Maclaurin series of $(1-x)^{-1/2}$ and $(1-x)^{1/2}$, for $|x|<1,$ can be written in the following form;

$$(1-x)^{-1/2}=1+\frac{1}{2}x+\frac{1\times3}{2\times4}x^2+\frac{1\times3\times5}{2\times4\times6}x^3+\frac{1\times3\times5\times7}{2\times4\times6\times8}x^4+O\left(x^5\right),$$

$$(1-x)^{1/2}=1-\frac{1}{2}x-\frac{1\times1}{2\times4}x^2-\frac{1\times1\times3}{2\times4\times6}x^3-\frac{1\times1\times3\times5}{2\times4\times6\times8}x^4-O\left(x^5\right).$$

Next, we consider $(1-2bti)^{-1/2}$ and $(1-2bti)^{1/2}$ in term of $(1-x)^{-1/2}$ and $(1-x)^{1/2}$ respectively, then the cumulant generating function of X becomes

$$\log\varphi_X(t)=\log\left[\frac{a}{a+1}+\frac{1}{a+1}\left(1+\frac{1}{2}(2bti)+\frac{1\times3}{2\times4}(2bti)^2\right.\right.$$

$$\left.\left.+\frac{1\times3\times5}{2\times4\times6}(2bti)^3+\frac{1\times3\times5\times7}{2\times4\times6\times8}(2bti)^4+\cdots\right)\right]$$

$$+a\left[1-\left(1-\frac{1}{2}(2bti)-\frac{1\times1}{2\times4}(2bti)^2\right.\right.$$

$$\left.\left.-\frac{1\times1\times3}{2\times4\times6}(2bti)^3-\frac{1\times1\times3\times5}{2\times4\times6\times8}(2bti)^4-\cdots\right)\right]$$

$$\approx\log\left[1+\frac{1}{a+1}\left((bti)+\frac{3}{2}(bti)^2+\frac{5}{2}(bti)^3+\frac{35}{8}(bti)^4\right)\right]$$

$$+a\left[(bti)+\frac{1}{2}(bti)^2+\frac{1}{2}(bti)^3+\frac{5}{8}(bti)^4\right],$$

and using the expansion

$$\log(1+x)=1+x-\frac{x^2}{2}+\frac{x^3}{3}-\frac{x^4}{4}+O\left(x^5\right),$$ we obtain

$$\log\varphi_X(t)$$

$$\approx\left[1+\frac{1}{a+1}\left((bti)+\frac{3}{2}(bti)^2+\frac{5}{2}(bti)^3+\frac{35}{8}(bti)^4\right)\right.$$

$$-\frac{1}{2}\left(\frac{1}{a+1}\right)^2\left((bti)^2+3(bti)^3+\frac{29}{4}(bti)^4\right)$$

$$\left.+\frac{1}{3}\left(\frac{1}{a+1}\right)^3\left((bti)^3+\frac{9}{2}(bti)^4\right)-\frac{1}{4}\left(\frac{1}{a+1}\right)^4\left((bti)^4+\cdots\right)\right]$$

$$+a\left[(bti)+\frac{1}{2}(bti)^2+\frac{1}{2}(bti)^3+\frac{5}{8}(bti)^4\right]$$

$$\approx1+\left[\left(\frac{1}{a+1}\right)+a\right](bti)+\left[\frac{3}{2}\left(\frac{1}{a+1}\right)-\frac{1}{2}\left(\frac{1}{a+1}\right)^2+\frac{1}{2}a\right](bti)^2$$

Suan Sunandha Science and Technology Journal

$$+\left[\frac{5}{2}\left(\frac{1}{a+1}\right)-\frac{3}{2}\left(\frac{1}{a+1}\right)^2+\frac{1}{3}\left(\frac{1}{a+1}\right)^3+\frac{1}{2}a\right](bti)^3$$
$$+\left[\frac{35}{8}\left(\frac{1}{a+1}\right)-\frac{29}{8}\left(\frac{1}{a+1}\right)^2+\frac{3}{2}\left(\frac{1}{a+1}\right)^3-\frac{1}{4}\left(\frac{1}{a+1}\right)^4+\frac{5}{8}a\right](bti)^4$$
$$\approx\left[\left(\frac{1}{a+1}\right)+a\right]\frac{(bti)}{1!}+\left[3\left(\frac{1}{a+1}\right)-\left(\frac{1}{a+1}\right)^2+a\right]\frac{(bti)^2}{2!}$$
$$+\left[15\left(\frac{1}{a+1}\right)-9\left(\frac{1}{a+1}\right)^2+2\left(\frac{1}{a+1}\right)^3+3a\right]\frac{(bti)^3}{3!}$$
$$+\left[105\left(\frac{1}{a+1}\right)-87\left(\frac{1}{a+1}\right)^2+36\left(\frac{1}{a+1}\right)^3-6\left(\frac{1}{a+1}\right)^4+15a\right]\frac{(bti)^4}{4!}.$$

From $K_X(t)=\log\varphi_X(t)=\sum_{n=1}^{m}\frac{\kappa_n}{n!}(ti)^n+O(t^{m+1})$,

the first four cumulants are given as follows:

$$\kappa_1=\left(\frac{1}{a+1}+a\right)b,$$
$$\kappa_2=\left(\frac{3}{a+1}-\frac{1}{(a+1)^2}+a\right)b^2,$$
$$\kappa_3=\left(\frac{15}{a+1}-\frac{9}{(a+1)^2}+\frac{2}{(a+1)^3}+3a\right)b^3,$$
$$\kappa_4=\left(\frac{105}{a+1}-\frac{87}{(a+1)^2}+\frac{36}{(a+1)^3}-\frac{6}{(a+1)^4}+15a\right)b^4, \quad \text{and}$$

the raw moments are related to the cumulants by the following formula:

$$E(X)=\kappa_1,$$
$$E(X^2)=\kappa_2+\kappa_1^2,$$
$$E(X^3)=\kappa_3+3\kappa_2\kappa_1+\kappa_1^3,$$
$$E(X^4)=\kappa_4+4\kappa_3\kappa_1+3\kappa_2^2+6\kappa_2\kappa_1^2+\kappa_1^4.$$

Substituting the cumulants in the equation above, we can find mean and variance are given by

$$E(X)=\left(\frac{1}{a+1}+a\right)b,$$

$$Var(X)=\kappa_2=\left(\frac{3}{a+1}-\frac{1}{(a+1)^2}+a\right)b^2.$$

Some mean and variance plots of the EMIG distribution with some parameter values are displayed in Figure 5.

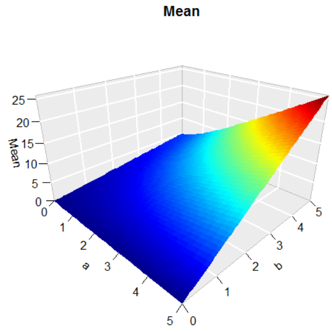

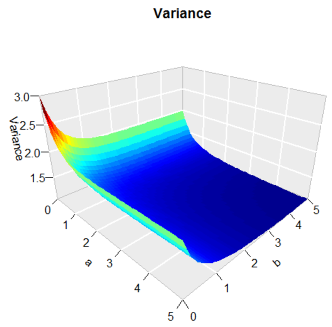

Figure 5. Mean and Variance of the EMIG distribution for difference values of (a,b).

3.1.2 Parameters estimation

The estimation of parameters for the extended mixture inverse Gaussian distribution via the Maximum Likelihood Estimation (MLE) procedure.The likelihood function of the distribution with parameters a and b is given by

$$L(a,b)=\prod_{i=1}^{n}\left\{\frac{1}{(a+1)b\sqrt{2\pi}}\left[a^2\left(\frac{b}{x_i}\right)^{3/2}+\left(\frac{b}{x_i}\right)^{1/2}\right]\times\exp\left[-\frac{1}{2}\left(\sqrt{\frac{x_i}{b}}-a\sqrt{\frac{b}{x_i}}\right)^2\right]\right\}$$

The log-likelihood function can be written as

$$\ell(a,b)=\log L(a,b)$$
$$=-n\log(ab+b)-\frac{n}{2}\log(2\pi)+na$$
$$-\frac{1}{2b}\sum_{i=1}^{n}x_i-\frac{a^2b}{2}\sum_{i=1}^{n}\frac{1}{x_i}$$
$$+\sum_{i=1}^{n}\log\left[a^2\left(\frac{b}{x_i}\right)^{3/2}+\left(\frac{b}{x_i}\right)^{1/2}\right]$$

Suan Sunandha Science and Technology Journal

$$
\begin{aligned}
&= -n\log\left(ab+b\right)-\frac{n}{2}\log\left(2\pi\right)+na \\
&\quad -\frac{1}{2b}\sum_{i=1}^{n}x_i-\frac{a^2b}{2}\sum_{i=1}^{n}\frac{1}{x_i} \\
&\quad +\sum_{i=1}^{n}\log\left[b^{1/2}x_i^{-3/2}\left(a^2b+x_i\right)\right] \\
&= -n\log\left(ab+b\right)-\frac{n}{2}\log\left(2\pi\right)+na \\
&\quad -\frac{1}{2b}\sum_{i=1}^{n}x_i-\frac{a^2b}{2}\sum_{i=1}^{n}\frac{1}{x_i}+\frac{n}{2}\log b-\frac{3}{2}\sum_{i=1}^{n}\log x_i \\
&\quad +\sum_{i=1}^{n}\log\left(a^2b+x_i\right).
\end{aligned}
$$

By taking first partial derivatives of the log-likelihood function each with respect to a and b, we obtain the equations;

$$\frac{\partial}{\partial a}\ell\left(a,b\right)=n-\frac{nb}{ab+b}-ab\sum_{i=1}^{n}\frac{1}{x_i}+\sum_{i=1}^{n}\frac{2ab}{a^2b+x_i},$$

$$
\begin{aligned}
\frac{\partial}{\partial b}\ell\left(a,b\right)&=\frac{-n\left(a+1\right)}{\left(ab+b\right)}+\frac{n}{2b}+\frac{1}{2b^2}\sum_{i=1}^{n}x_i \\
&\quad -\frac{a^2}{2}\sum_{i=1}^{n}\frac{1}{x_i}+\sum_{i=1}^{n}\frac{a^2}{a^2b+x_i}.
\end{aligned}
$$

The MLE solutions of $\hat{a},\hat{b}$ can be obtained by equating the above equations to zero and solving the resulting equations simultaneously using a numerical procedure with the Newton-Raphson method in R (R Development Core Team, 2015).

3.2 Numerical Result

In this section, the EMIG distribution is applied on real data set which is taken from Gupta and Kundu (2009) which represent final examination marks in mathematics of the slow pace students in 2003, The data are given in Table 1.

Table 1. The final examination marks in mathematics of the slow pace students in 2003.

29	25	50	15	13	27	15	18
7	7	8	19	12	18	5	21
15	86	21	15	86	21	15	14
70	44	6	23	58	19	50	23
11	6	34	18	28	34	12	37
4	60	20	23	40	65	19	31

For this data, we have that mean=25.89 and variance= 345. We have fitted the EMIG, MIG, IG, LBIG and BS distributions to this data set by using maximum likelihood estimation. We obtain the estimates parameters and AIC statistics for all distributions are shown in Table 2. Next, we compute Anderson-Daring (AD) test for goodness of fit distribution to these data which are shown in Table 3.

Table 2. MLE of the model parameters for the marks data set.

Distribution	**Estimate parameters**			**AIC**
	a	b	p	
EMIG	1.73	12.34	-	388.74
MIG	5.61	12.03	0.74	918.49
IG	5.60	12.08	-	916.50
LBIG	1.54	10.20	-	396.31
BS	5.84	10.67	-	916.11

Distribution	**Estimate parameters**			**AIC**
	a	b	p	
EMIG	1.73	12.34	-	388.74
MIG	5.61	12.03	0.74	918.49
IG	5.60	12.08	-	916.50
LBIG	1.54	10.20		396.31
BS	5.84	10.67	-	916.11

Table 3. Goodness of fit test for the marks data set by using Anderson-Darling test

Distribution	**AD test**	
	Statistic	**P-value**
EMIG	0.3215	0.9208
MIG	0.1633	0.0107
IG	0.3529	0.8935
LBIG	0.3154	0.9109
BS	0.3279	0.9156

The P-value of Anderson-Darling test is shown that the EMIG distribution performs better than MIG, IG, LBIG and BS distributions and the value of AIC statistic is shown that the EMIG distribution is the best fit for this data. The fitted probability density functions and the observed histograms are given in Figure 6.

Suan Sunandha Science and Technology Journal

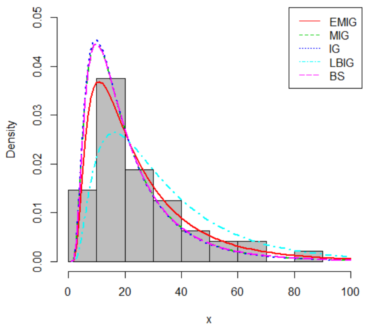

Figure 6. Histogram of the marks data.

4. Conclusion

In this paper, we have presented the EMIG distribution which is given by adding a new weight parameter to the MIG distribution. The BS and LBIG distribution are some special case of EMIG. We mainly studied the statistical properties of EMIG distribution such as pdf, density function, survival function, hazard rate function, cumulants, the first four moments, mean and variance. We discuss the estimation of the parameters by maximum likelihood. Finally, we compare the fit of the EMIG distribution with MIG, IG, LBIG and the BS distributions by using marks data. The AIC statistics indicates that the EMIG is best fit for real data.

Acknowledgement

The author would like to thank the editor and referee for their useful comments and suggestions which considerably improved this article.

References

Akman, O., & Gupta, R.C. (1992). A comparison of various estimators of an inverse Gaussian distribution. *Journal of Statistical Computation and Simulation*,*40*,1-2,71-81. doi:10.1080/0094 9659208811366.

Balakrishnan, N., Leiva, V., Sanhueza, A. & E. Cabrera, (2009). Mixture inverse Gaussian distributions and its transformations, moments and applications. *Statistics*, *43*(1), 91-104, doi: 10.1080/02331880701829948.

Gradshteyn, I.S., & Ryzhik, I.M. (2007). *Table of integrals, series, and products.* (7th ed.). MA, USA: Elsevier Academic Press.

Gupta, R.C., & Akman, H.O. (1995). On the reliability studies of a weighted inverse Gaussian model. *Journal of Statistical Planning and Inference*, *48* (1), 69-83, doi:10. 1016/0378-3758(94)00148-O.

Gupta, R.D., & Kundu, D. (2009). A new class of weighted exponential distributions, *Statistics: A Journal of Theoretical and Applied Statistics*, *43*(6), 621-634, doi:10.1080/023318 80802605346.

Gupta, R.C., & Kundu, D. (2011). Weighted inverse Gaussian a versatile life time model. *Journal of Applied Statistics*, *38*(12), 2695-2708, doi:10.1 080/02664763.2011.567251.

Henze, N., & Klar, B. (2002). Goodness-of-fit tests for the inverse Gaussian distribution based on the empirical laplace transform. *Annals of the Institute of Statistical Mathematics*, *54*(2), 425-444, doi:10.1023/A:1022442506681.

Jorgensen B., Seshadri, V., & Whitmore, G.A. (1991). On the mixture of the inverse Gaussian distribution with its complementary reciprocal. *Scandinavian Journal of Statistics*, *18*(1), 77-89.

R Development Core Team, (2015). *A language and environment for statistical computing. R foundation for statistical computing*, Vienna, Austria.

Von Alven, W.H., (1964). *Reliability Engineering*. New Jersey: prentice-hall Inc.

Available online at http://www.ssstj.sci.ssru.ac.th

Suan Sunandha Science and Technology Journal

Effect of Carboxyl-Terminal Truncation on the Catalytic Performance of D-Phenylglycine Aminotransferase

Aiya Chantarasiri [1*], Rachael Patterson[2], Vithaya Meevootisom[2], Suthep Wiyakrutta[2]

[1]Faculty of Science, Energy and Environment, King Mongkut's University of Technology North Bangkok, Rayong Campus, Rayong 21120, Thailand

[2] Department of Microbiology, Faculty of Science, Mahidol University, Bangkok 10400, Thailand

Corresponding authors E-mail: * aiya.c@sciee.kmutnb.ac.th

Abstract: The D-phenylglycine aminotransferase (D-PhgAT) is a novel enzyme that can be used to synthesize precursors of antibiotics. This research addressed the function of the carboxyl-terminal (C-terminal) of D-PhgAT. Its C-terminal amino acid sequence was compared to other related proteins using bioinformatics tools. The analyzed amino acid sequence was used to produce a genetically modified enzyme having a truncation of the 10 amino acid residues at the C-terminal region. The truncated D-PhgAT was purified and analyzed for catalytic performance. The results revealed that the truncated enzyme had better catalytic performance than the full-length enzyme by 37.49%. This research is a preliminary study for improving the enzymatic performance of D-PhgAT by structure-guided engineering and can be applied in the development of other enzymes.

Keywords: D-phenylglycine aminotransferase, Carboxyl-terminus, Catalytic performance, Bioinformatics tools.

1. Introduction

D-phenylglycine (D-Phg) and its derivative, D-4-hydroxyphenylglycine (D-HPG), are important precursors used in the preparation of semi-synthetic penicillin and cephalosporin antibiotics. These precursors can be prepared by microbial enzymes (Müller et al., 2006). At present, a novel enzyme D-phenylglycine aminotransferase (D-PhgAT) (EC 2.6.1.72), isolated from Thai soil bacterium *Pseudomonas stutzeri* ST-201 (Wiyakrutta & Meevootisom, 1997), has the potential for producing D-Phg and D-HPG using a low-cost and simple process. D-PhgAT is a pyridoxal-5'-phosphate (PLP) dependent enzyme composed of two identical sub-units with a molecular weight of 47,500 Da each (Figure 1). It catalyzes a reversible stereo-inverting transamination of D-Phg or D-HPG with 2-oxoglutaric acid as the amino group acceptor, resulting in the formation of L-glutamic acid and benzoylformic acid (BZF) or 4-hydroxy-BZF (Figure 2). D-PhgAT could be applied in the preparation of D-Phg or D-HPG, the important side chain building blocks of semi-synthetic penicillin and cephalosporin, such as ampicillin and cephalexin, in only a single enzymatic reaction step using a low-cost amino donor as L-glutamic acid. Moreover, D-PhgAT has been used in analytical and pharmaceutical applications, such as for the determination of L-glutamate and monosodium glutamate (MSG) in various foods by spectrophotometric enzymatic cycling method with L-glutamate dehydrogenase (Khampha et al., 2004) and the quantitative determination of amoxicillin by UV-spectrophotometric method with penicillin acylase (Rojanarata et al., 2010).

Due to the benefits mentioned above, D-PhgAT has been studied and genetically engineered for improving enzymatic performance. Many studies have reported that truncation of some amino acid residues at the carboxyl-terminus (C-terminus) of target enzymes can enhance their thermal stability (Vihinen et al., 1994; Ohdan et al., 1999; Liao et al., 2002), solubility (Krueger et al., 2006) and specific activity (Lee et al., 1997; Sanoja et al., 2000). The lecithin-cholesterol acyltransferase was truncated at the C-terminus of 5 amino acid residues (Lee et al., 1997) and the specific activity of the truncated mutant was increased 8-fold.

Suan Sunandha Science and Technology Journal

Figure 1. Three-dimensional structure of D-PhgAT, consisting of two identical subunits (Chains A and A′). Red region represents the 10 amino acid residues at each C-terminus. The diagram was generated from the crystal structure data of D-PhgAT (PDB ID: 2CYB) using ICM-Browser 3.7 software.

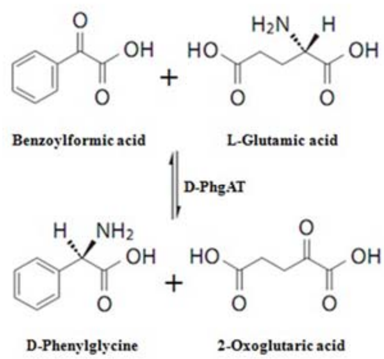

Figure 2. Stereo-inverting transamination reaction of D-PhgAT. The diagram was modified from Chantarasiri et al. (2012)

To address the function of the C-terminus on the catalytic performance of D-PhgAT, the C-terminal truncated enzyme was constructed using structure-guided engineering and monitored for the resulting effect.

2. Materials and Methods

2.1 In silico analyses

The target amino acid region for C-terminal truncation was predicted by bioinformatics tools. A comparison of amino acid sequences between D-PhgAT (GenBank Accession number: AAQ82900.1) and other related proteins in the National Center for Biotechnology Information (NCBI) database was completed employing a BLAST program (Altschul et al., 1990). The 3D Similarity program (Prlić et al., 2010; Ye and Godzik, 2003) was applied on the three-dimensional structure of D-PhgAT (PDB ID: 2CY8) to compare the identity with other enzymes in the RCSB Protein Data Bank (PDB). The intimated enzymes from databases were chosen for amino acid sequence alignment. The sequences were aligned focusing on the C-terminal region by ClustalW 2.1 program (Larkin et al., 2007).

2.2 Construction of C-terminal truncated D-PhgAT

Plasmid pEPL, carrying the *dpgA* gene (GenBank Accession number: AY319935.1) encoding the full-length D-PhgAT from *Pseudomonas stutzeri* ST-201, was kindly provided by Dr. Poramaet Laowanapiban. The *dpgA* gene was genetically modified by QuikChange® Lightning Mutagenesis Kit (Agilent Technologies, USA) according to the prediction provided by bioinformatics analyses. To amplify the modified *dpgA* gene, a forward primer (5'-GACGAAAACCT GTTGTCTTGGTGAAAACTAGCCTGAAACTT G-3') and a reverse primer (5'-CAAGTT TCAGGCTAGTTTTCACCAAGACAACAGGTT TTCGTC-3') were designed using QuikChange® Primer Design Program. DNA sequencing of the modified *dpgA* gene was completed at Macrogen Inc., Korea. The modified *dpgA* gene encoding the C-terminal truncated D-PhgAT was placed under the controlled expression system of the pET-17b plasmid (Novagen, Germany) and expressed in expression host *Escherichia coli* BL 21 (DE3).

2.3 Overexpression and purification of D-PhgAT

The full-length D-PhgAT was prepared as described previously (Kongsaeree et al., 2003). For expression of the C-terminal truncated D-PhgAT, *E. coli* BL 21 (DE3) cells containing the modified *dpgA* gene were cultured in LB-Miller broth (Difco, USA) supplemented with 50 µg/ml of ampicillin at 37°C with 200 rpm shaking until an OD_{600} of 0.6 was achieved. Isopropyl β-D-1-thiogalactopyranoside (IPTG) was added to the final concentration of 0.4 mM to induce C-terminal

Suan Sunandha Science and Technology Journal

truncated D-PhgAT expression. Induced *E. coli* cells were further incubated for 16 hours at 20°C with 100 rpm shaking. The induced cells were harvested by centrifugation. The pellet of induced cells was re-suspended in 9 volumes of 20 mM TEMP buffer (pH 7.6) (Chantarasiri et al., 2012) and disrupted by ultra-sonication. Crude enzyme solution was clarified by centrifugation and purified by ammonium sulfate precipitation at 25-45% saturation, followed by hydrophobic interaction chromatography on a Phenyl agarose (CL-4B) column (Amersham Pharmacia Biotech, Sweden) and a DEAE sepharose anion-exchange column (GE Healthcare, Sweden). All chromatography was carried out on a BioLogic Controller Fast Protein Liquid Chromatography system (BIO-RAD, USA). The active fractions were combined and concentrated using Amicon Ultra-15 (30 kDa) centrifugal filter devices (Millipore, Ireland). The purity of enzymes was determined by SDS-PAGE and the concentration was determined by Bradford assay (Bradford et al., 1976) using bovine serum albumin (BSA) as the standard. The purified enzymes were kept at 4°C in Protein LoBind tubes until use (Eppendorf, Germany).

2.4 D-PhgAT activity assay

The D-PhgAT activity assay was determined using a kinetic spectrophotometric method in the direction of 4-hydroxy-BZF formation as described previously (Chantarasiri et al., 2012). The 1,000-µl volume of reaction mixture contained 20 µl of appropriate diluted D-PhgAT, 10 mM D-HPG, 10 mM 2-oxoglutaric acid, 50 mM CAPSO buffer (pH 9.5), 5 µM PLP and 5 µM EDTA. The rate of 4-hydroxy-BZF formation was measured as a function of time by monitoring the increase in absorbance at 340 nm for a 180-s time period using a Heλios spectrophotometer (Spectronic Unicam, UK). The measurements were performed in triplicate. One unit (U) of D-PhgAT activity was defined as the amount of the enzyme required to release 1 µmol of 4-hydroxy-BZF per 1 min under specific reaction conditions, with 1 unit of specific activity (U/mg) defined as the activity of D-PhgAT per milligram of total enzyme.

3. Results and Discussions

3.1 Target region for D-PhgAT truncation at C-terminal end

Bioinformatics analyses revealed that D-PhgAT had an amino acid sequence closely related to glutamate-1-semialdehyde 2, 1-aminomutase (EC 5.4.3.8; GenBank Accession number: WP_010046875.1) with 43% identity. The three-dimensional structure of D-PhgAT was nearly identical to glutamate-1-semialdehyde 2, 1-aminomutase (PDB ID: 2ZSL) with 21% identity and β-phenylalanine aminotransferase (PDB ID: 4AO9) with 19% identity, respectively. The amino acid sequence alignment of three intimated enzymes was done by Clustal W program. D-PhgAT was longer than glutamate-1-semialdehyde 2, 1-aminomutase at the C-terminal end by 15 amino acid residues and β-phenylalanine aminotransferase by 10 amino acid residues. To avoid any unfavorable effect on the three-dimensional structure, activity and stability of D-PhgAT from abundant amino acid truncation (Vihinen et al., 1994), only 10 amino acid residues from position Q444 to S453 (Q444-P445-T446-N447-L448-S449-G450-N451-Q452-S453) at each C-terminus of D-PhgAT subunit were preferred for truncation. The predicted region for truncation at the C-terminus of D-PhgAT is shown as red in Figure 1.

3.2 Effect of C-terminal truncation on overexpression and enzyme purity

E. coli BL21 (DE3) cells containing the modified *dpgA* gene could be induced and expressed the C-terminal truncated D-PhgAT. It was evident that the designed engineering had no unfavorable effect on the expression or folding processes of D-PhgAT in expression host. The purity of D-PhgAT, with a molecular weight of 47.5 kDa, is shown in Figure 3.

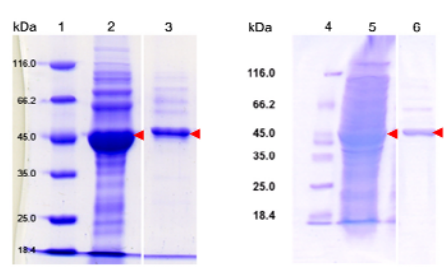

Figure 3. SDS-PAGE analysis of D-PhgAT after the purification processes. Lanes 1 and 4 were the

Suan Sunandha Science and Technology Journal

protein markers with molecular weight (Fermentas, USA). Lanes 2 and 3 were a crude enzyme solution and purified full-length enzymes, respectively. Lanes 5 and 6 were a crude C-terminal truncated enzyme solution and purified C-terminal truncated enzymes, respectively.

3.3 Effect of C-terminal truncation on enzyme activity

The catalytic performance of full-length and C-terminal truncated D-PhgAT was monitored in the direction of 4-hydroxy-BZF formation. The specific activity was 63.89 ± 2.39 U/mg for full-length D-PhgAT and 87.84 ± 0.04 U/mg for the C-terminal truncated enzyme. The truncation of 10 amino acid residues at C-terminus had a positive effect on the catalytic performance of D-PhgAT by 37.49%. Other previous studies have discussed truncation at the C-terminus of the target enzymes as having increased slightly or causing no negative effect on catalytic performance (Evans et al., 1990; Ohdan et al., 1999; Sanoja et al., 2000; Lin et al., 2009). For D-PhgAT, the 10 amino acid residues at the C-terminal end (the position Q444 to S453) were far apart from the active site and catalytic domain. However, how is it possible that they improved the catalytic performance? The explanation is supported by a previous study (Chantarasiri et al., 2012), which showed that the Q444 residue in the C-terminal region of D-PhgAT was the highly solvent exposed residues and involved in crystal contact residues. The crystal contact is an intermolecular interface that is critical to holding the protein molecule together when forming a protein crystal and protein aggregation (Chantarasiri et al., 2012). The Q444 residue is able to form the hydrogen bonds that interact with amino acid residues of different D-PhgAT subunits, such as K10 and D55 (Figure 4) (Chantarasiri et al., 2012). This interaction results in protein aggregation and protein precipitation that shows no catalytic performance after the protein purification processes. The truncation of 10 amino acid residues, which includes the Q444 residue at the C-terminal region of D-PhgAT, could abolish protein-protein interactions and prevent protein aggregation after protein purification processes, resulting in the increased catalytic performance of D-PhgAT in the solution.

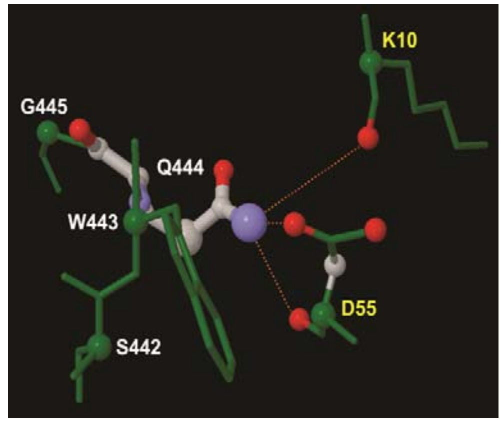

Figure 4. In silico predicted crystal contacts between Q444 and K10/D55 from another D-PhgAT molecule (red dotted line denotes hydrogen bonds). The diagram was modified from Chantarasiri et al (2012).

4. Conclusions

We have shown an approach for increasing the catalytic performance of D-PhgAT by truncation of 10 amino acid residues at the C-terminal region guided by bioinformatics prediction for amino acid sequence and three-dimensional structure. With the development of nucleotide and protein databases, knowledge from this study could be applied to develop and improve the catalytic performance of other enzymes.

Acknowledgements

We are grateful to Dr. Poramaet Laowanapiban (M.D., Ph.D.) for kindly providing the plasmid pEPL.

References

Altschul, S. F., Gish, W., Miller, W., Myers, E. W., & Lipman, D. J. (1990). Basic local alignment search tool, *Journal of Molecular Biology*, *215*, 403-410.

Bradford, M. M. (1976). Rapid and sensitive method for the quantitation of microgram quantities of protein utilizing the principle of protein-dye binding, *Anal Biochemistry*,*72*, 248-254.

Chantarasiri, A., Meevootisom, V., Isarangkul, D., &Wiyakrutta, S. (2012). Effective improvement of D-phenylglycine aminotransferase solubility

Suan Sunandha Science and Technology Journal

by protein crystal contact engineering, *Journal of Molecular Microbiology ND Biotechnology*, *22*(3), 147-155. doi: 10.1159/000339833.

Evans, R., Ford, C., Sierks, M., Nikolov, Z., & Svensson, B. (1990). Activity and thermal stability of genetically truncated forms of *Aspergillus glucoamylase*, *Gene*, *91*(1), 131-134.

Khampha, W., Meevootisom, V., & Wiyakrutta, S. (2004). Spectrophotometric enzymatic cycling method using L-glutamate dehydrogenase and D-phenylglycine aminotransferase for determination of L-glutamate in foods, *Analytica Chimica Acta*, *520*, 133-139.

Kongsaeree, P., Samanchart, C., Laowanapiban, P., Wiyakrutta, S., & Meevootisom, V. (2003). Crystallization and preliminary X-ray crystallographic analysis of D-phenylglycine aminotransferase from *Pseudomonas stutzeri* ST201, *Acta Crystallographica Section D*, *59*, 953-954.

Krueger, S. K., Siddens, L. K., Henderson, M. C., Van Dyke, J. E., Karplus, P. A., Pereira, C. B., & Williams, D. E. (2006). C-terminal truncation of rabbit flavin-containing monooxygenase isoform 2 enhances solubility, *Archives of Biochemistry and Biophysics*, *450*, 149-156.

Larkin, M. A., Blackshields, G., Brown, N. P., Chenna, R., McGettigan, P. A., McWilliam, H.,…Higgins, D. G. (2007). Clustal W and Clustal X version 2.0, *Bioinformatics*, *23*, 2947-2948.

Lee, Y. P., Adimoolam, S., Liu, M., Subbaiah, P. V., Glenn, K., & Jonas, A. (1997). Analysis of human lecithin-cholesterol acyltransferase activity by carboxyl-terminal truncation, *Biochimica et Biophysica Acta*, *1344*, 250-261.

Liao, J. H., Lee, J. S., & Chiou, S. H. (2002). C-terminal lysine truncation increases thermostability and enhances chaperone-like function of porcine αB-crystallin, *Biochemical and Biophysical Research Communications*, *297*, 309-316.

Lin, F. P., Chuang, H. H., Liu, Y. H., Hsieh, C. Y., Lin, P. W., & Lin, H. Y. (2009). Effects of C-terminal amino acids truncation on enzyme properties of *Aeromonas caviae* D1 chitinase, *Archives of Microbiology*, *191*(3), 265-273.

Müller, U., Assema, F., Gunsior, M., Orf, S., Kremer, S., Schipper, D.,…Wubbolts, M. (2006). Metabolic engineering of the *E. coli* L-phenylalanine pathway for the production D-phenylglycine (D-Phg), *Metabolic Engineering, 8*, 196-208.

Ohdan, K., Kuriki, T., Kaneko, H., Shimada, J., Takada, T., Fujimoto, Z., Mizuno, H., & Okada, S. (1999). Characteristics of two forms of α-amylases and structural implication, *Applied and Environmental Microbiology*, *65*(10), 4652-4658.

Prlić, A., Bliven, S., Rose, P. W., Bluhm, W. F., Bizon, C., Godzik, A., & Bourne, P. E. (2010). Pre-calculated protein structure alignments at the RCSB PDB website, *Bioinformatics*, *26*, 2983-2985.

Rojanarata, T., Ngawhirunpat, T., Saehuan, C., Wiyakrutta, S., & Meevootisom, V. (2010). A simple, sensitive and green bi-enzymatic UV-spectrophotometric assay of amoxicillin formulations, *Enzyme and Microbial Technology*, *46*, 292-296.

Sanoja, R. R., Morlon-Guyot, J., Jore, J., Pintado, J., Juge, N., & Guyot, J. P. (2000). Comparative characterization of complete and truncated forms of *Lactobacillus amylovorus* α-amylases and role of the C-terminal direct repeats in raw-starch binding, *Applied and Environmental Microbiology*, *66*(8), 3350-3356.

Vihinen, M., Peltonen, T., Iitiä, A., Suominen, I., & Mäntsälä, P. (1994). C-terminal truncations of a thermostable *Bacillus stearothermophilus* alpha-amylase, *Protein Engineering*, *7*(10), 1255-1259.

Wiyakrutta, S., & Meevootisom, V. (1997). A stereo-inverting D-phenylglycine aminotran-sferase from *Pseudomonas stutzeri* ST-201: purification, characterization and application for D-phenylglycine synthesis, *Journal of Biotechnology, 55*, 193-203.

Ye, Y., & Godzik, A. (2003). Flexible structure alignment by chaining aligned fragment pairs allowing twists, *Bioinformatics*,*19*, 245-255.

Available online at http://www.ssstj.sci.ssru.ac.th

Suan Sunandha Science and Technology Journal

Flood Hazard Mapping using Hydraulic Model and GIS: A Case Study in Mandalay City, Myanmar

Kyu Kyu Sein[1*], Thida Myint[2]

[1,2]Department of Meteorology and Hydrology, Ministry of Transport
Office No.5, Ministry of Transport, Nay Pyi Taw, Myanmar

Corresponding author E-mail: *sein.dmhmdy@gmail.com

Abstract: This paper presents the use of flood frequency analysis integrating with 1D Hydraulic model (HEC-RAS) and Geographic Information System (GIS) to prepare flood hazard maps of different return periods in Ayeyarwady River at Mandalay City in Myanmar. Gumbel's distribution was used to calculate the flood peak of different return periods, namely, 10 years, 20 years, 50 years, and 100 years. The flood peak from frequency analysis were input into HEC-RAS model to find the corresponding flood level and extents in the study area. The model results were used in integrating with ArcGIS to generate flood plain maps. Flood depths and extents have been identified through flood plain maps. Analysis of 100 years return period flood plain map indicated that 157.88 km^2 with the percentage of 17.54% is likely to be inundated. The predicted flood depth ranges varies from greater than 0 to 24 m in the flood plains and on the river. The range between 3 to 5 m were identified in the urban area of Chanayetharzan, Patheingyi, and Amarapua Townships. The highest inundated area was 85 km^2 in the Amarapura Township.

Keywords: Flood frequency, HEC-RAS, Flood hazard, Return period, GIS.

1. Introduction

Myanmar is one of the vulnerability to climate change impacts in terms of extreme temperature, severe drought, cyclones, floods, heavy rainfall and less precipitation, landslides, earthquakes and tsunami. Flooding is the second largest natural disaster after a fire, which is facing every year in Myanmar (Union of Myanmar, et al., 2009). Flooding is negatively impacting on social economy, loss of lives and properties, health related problems, and ecosystem functions. In Myanmar, there are two types of flood; widespread flood and flash flood which mainly occur in the month of July, August and late September to October in each year (DMH, 2004). The maximum flood peak can be seen in August due to evidence of peak monsoon rains. The main cause of river flooding is the occurrence of intense rainfall during the monsoon season in the northern part and eastern part of Myanmar, which are the upstream of the rivers (DMH, 2010). According to the historical data from DMH, the percentages of occurrence of floods which exceeded the danger level in medium and large rivers of Myanmar are 6% in June, 23% in July, 49 % in August, 14% in September and 8% in October (Aye Ko, 2006). The floods of 2015, 2004, 1974, 1997, 1991, 1973, and 1988 (years are arranged with respect to their intensities) verify their devastating nature and destructive impact on infrastructure in Myanmar (Sein, 2012).

In 2015, Myanmar experienced in unexpected big floods affecting the entire country. A total of 69 people have been killed and over 259,000 people, including 88,000 children, 39,474 households were affected, more than 4046.85 km^2 of farmland were inundated, with some 2104.36 km^2 were damaged across 12 of Myanmar's 14 States and Regions since the monsoon onset rains in June (UNOCHA, 2015). Due to this phenomenon, it is necessary to evaluate flood hazard assessment in order to know how much would be inundated and destroyed if a particular hazard occurs.

One of the widely used models of analysis, flood plain delineation is the HEC-RAS hydraulic model developed by the US Army Corps of Engineers. This model results give to determine the extent of inundation, and flood depth (Brunner and Bonner, 2010). The combination with HEC-RAS model and GIS environment allow to analyze and visualize of floodplain management and accessing the changing of water surface profile (Brunner and Bonner, 2010; Shahzad, et al., 2015). Moreover, GIS environment performs as the effective planning tool

Suan Sunandha Science and Technology Journal

to export data result from HEC-RAS model to floodplain management, damage analysis, and flood early warning systems (Tate and Maidment, 1999). The input parameters to HEC-RAS models are river discharge, channel, flood plain geometry, and channel resistance. The objective of this study intends to delineate a flood hazard map in the Ayeyarwady River at Mandalay city in Myanmar by integrating 1D hydraulic model and GIS environment in order to provide decision makers and relevant agencies to protect flood disaster.

2. Reviews of past flood in Mandalay city

In 2004, the flood has occurred a result of intense rainfall in the upper portion of the Ayeyarwwady River. The highest recorded water level of Ayeyarwady River was 1382 cm during the study period 1968-2010 and it exceeded 122 cm above danger level. The people living, in near the river have been moving out of their homes and staying in refugee camps located on higher place. The agricultural areas of 122.68 km^2 were damaged out of 329.90 km^2 were inundated (DMH, 2004).

In 2006, flooding was facing two times. In September it was tropical cyclone in the South China Sea and low pressure in the Bay of Bengal that caused heavy continuous rains in the study area. Heavy rains continued throughout 2nd September to 30th September and accumulated 450 mm of rainfall which was the half of the normal annual rainfall recorded in the past 60 years. Therefore, the local drainage system cannot control the excess amount of higher surface runoff and overflow to the surrounding area. As the result, at least 20 people were killed and 4000 people left their home. The second flooding in October was due to the overflowing of Myitnge River. The highest recorded water level of Myitnge River was 1048 cm during the study period and it exceeded 178 cm above danger level (DMH, 2006).

In 2010 and 2011 flood were not totally related with River flooding. The urban area such as Aungpinlay,Aungtharyar,Thamankhone,Kywesakn, Nyaung Kawe and Patheingyi area were flooded caused by torrential rain during the month of October. These floods destroyed thousands of homes, 3,000 people had to leave their homes, and 10 people including 7 children were killed, and almost 2,000 people got injuries (DMH, 2010 and 2011).

3. Materials and Method

3.1 Study Area

Mandalay city is situated in the Mandalay region of the central component of Myanmar latitude of 21º 45'- 22º 10' N and longitude of 96º 00'- 96º 21' E. It lies on the eastern bank of the Ayeyarwady River. The study area covers an area of about 900 km^2 with 7 townships namely Aungmyaetharzan, Chanayetharzan, Chanmya-tharzi, Mahaaungmyae, Pyigyitagon, Amarapura and Patheingyi (Figure 1).

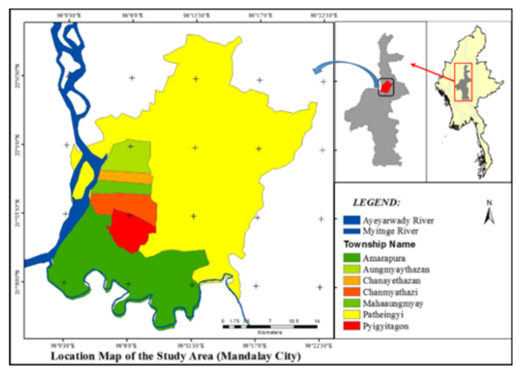

Figure 1. Location map of Mandalay city.

Among the 7 townships, most part of the area of Amarapura and Patheingyi or rural area which has more than 4.04 km^2 of farmland and the remaining 5 townships are urban area. The lowest elevation range can be seen in and around Ayeyarwady River, western part of the city and the highest elevation is the eastern part of the city which has mountains. As Mandalay is the second largest city as same as the population. The climate in the study area is normally hot and dry climate and annual rainfall of 500 mm to 1500 mm. The normal rainfall is 811 mm. The pattern of rainfall distribution throughout the year is two peaks, once in May and the other in September due to the influence of monsoon onset and withdraw. The Ayeyarwady River and one of its tributaries, Myitnge River is passing through in the study area. The original of the Ayeyarwady River is Tibetan Plateau and the total catchment area is 2,445,434km^2 and its length is about 1600 km from origin to its river mouth (DMH, 2004). The catch-

Suan Sunandha Science and Technology Journal

ment area of Ayeyarwady River in Mandalay is 120,190 km^2 with maximum discharge 30216 m^3/sec while Myitnge River in Mandalay is 27,904 km^2 with maximum discharge 665 m^3/sec. During the study period 1968-2010, the flood was observed in 12 years in the Ayeyarwady River with maximum peak in August and 36 years in Myitnge River with maximum peak in July (Aye Ko, 2006). The comparison between monthly mean rainfall and water level of the two rivers are shown in figure (Figure 2). Rainfall peak and water level peak are different since local rain is not affected in the study area. Most of the flood in the study area is mainly related to upstream rain effects.

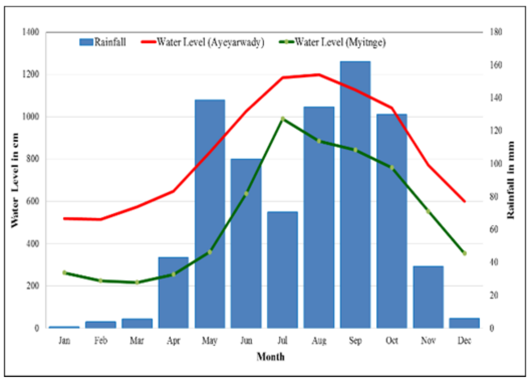

Figure 2. Monthly highest water level of two rivers compared with monthly maximum rainfall in the study area.

3.2 Data

Annual maximum water level and peak discharge data of 1968 – 2010 were collected from the Department of Meteorology and Hydrology to calculate the different return periods of 10 years, 20 years, 50 years, and 100 years. The 30 m resolution of Advanced Space borne Thermal Emission and Radiometer (ASTER) Digital Elevation Model (DEM) (Figure 3) was freely downloaded from the website gdem.ersdac.jspacesystem.or.jp in order to extracts basin geometry, stream networks, river geometry, Triangular Irregular Network (TIN), and flow direction. The UTM 50,000 scale topographic maps were collected from the Mandalay City Development Committee to digitize the study area and drainage system.

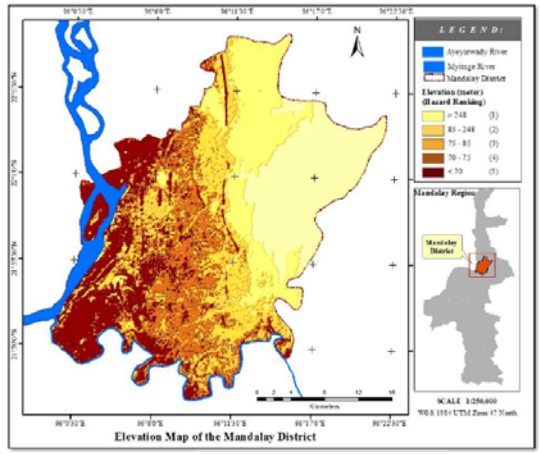

Figure 3. Elevation range in the study area.

3.3 Method

3.3.1 Flood Frequency Analysis

The Gumbel's distribution method was used to analyze the extreme values of different return periods of 10 years, 20 years, 50 years and 100 years using observed discharge data. In this method the variate X (maximum rainfall or flood peak discharge) with a recurrence interval T is given by (Subramanya, 1994);

$$x_T = \bar{x} + K\sigma_{n-1} \tag{1}$$

Where, x_T = maximum rainfall or flood peak discharge or water level

$\bar{x}$ = average value of x

σ_{n-1} = standard deviation of sample size N

$$\sigma_{n-1} = \sqrt{\frac{\Sigma(x-\bar{x})^2}{N-1}} \tag{2}$$

K = frequency factor expressed as

$$K = \frac{y_T - \bar{y}_n}{S_n} \tag{3}$$

y_T = reduced variate, a function of T and is given by

$$y_T = -\left[\ln.\ln\frac{T}{T-1}\right] \tag{4}$$

$\bar{y}_n$ = reduce mean, a function of sample size N

S_n = reduce standard deviation, a function of sample size N

Suan Sunandha Science and Technology Journal

3.3.2 Flood plain analysis using HEC-RAS and GIS

ASTER DEM was used as input data to generate watershed and drainage network in HEC-GeoRAS. The channel, bank stations, flow direction and cross section cutlines were prepared in HEC-GeoRAS and exported to HEC-RAS model. Upstream (Thabeikkyin) and Downstream (Sagaing) stations of Mandalay were selected for flow input data. The different return periods of flood peak were obtained from Gumbel's and used as an input to HEC-RAS model in order to simulate results for each cross section.

At the same time, water surface profiles were running in the model for 10, 20, 50 and 100 years flood. After running input data in HEC-RAS model, the result outputs were exported to ArcGIS in the format of RAS GIS Export file. The RAS GIS Export File was imported into ArcGIS after generating water surface and flood plain delineation. ArcGIS was used to generate flood depth and inundation mapping for different return periods. The overall methodology flow chart is shown in (Figure 4).

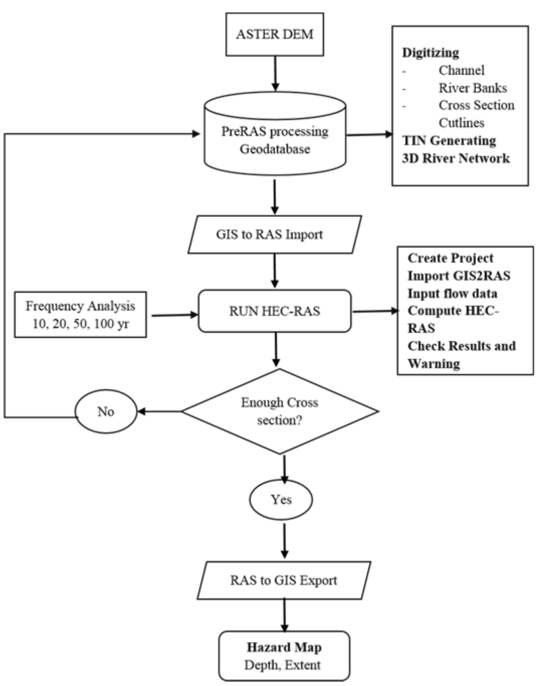

F

Figure 4. Methodology flow chart for flood hazard mapping.

4. Results and Discussion

Flood hazard maps for the different return periods of 10, 20, 50, 100 years were conducted using the annual peak flow of 43 years from 1968 to 2010. The maximum discharges at upstream and downstream for different periods were obtained using Gumbel's distributions (Table 1).

Table 1. Peak Discharge Data of Upstream and Downstream.

Return Periods	Upstream		Downstream	
	Flow (m^3/s)	Water Level (m)	Flow (m^3/s)	Water Level (m)
10 yrs	25194	82.39	31037	69.94
20 yrs	27008	83.06	33390	70.34
50 yrs	29356	83.87	36309	70.76
100 yrs	31116	84.43	38495	71.14

Although the different return periods, namely 10, 20, 50, and 100 years flood plain maps were generated, but only the 100 years flood plain maps are presented for Mandalay city (Figure 5). Since peak flow of 100 years recurrent interval is much higher and more reliable than the other recurrent interval. The model results showed that 17.54% area is predicted to be inundated under 100 years return period (Table 2) under different flood depths. The depths range in 100 years flood varies from greater than 0 to 24 m in the flood plains and on the river. The affected area under various flood depths is shown in (Figure 6). The total inundated area in Mandalay is 157.88 km^2.

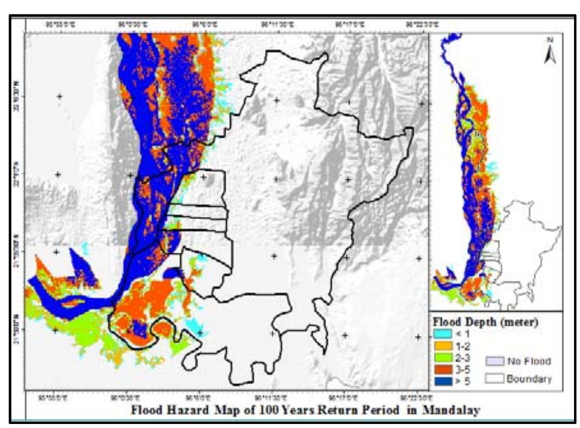

Suan Sunandha Science and Technology Journal

Figure 5. 100 years flood hazard map I Mandalay City.

Table 2. Percentage flood affected area for 100 years return period flood.

Water Depth(m)	100 years	
	Flood Area (km^2)	% of flood effected Area
< 1	14.30	1.59
1-2	9.92	1.10
2-3	10.52	1.17
3-5	53.64	5.96
> 5	69.50	7.72
Total	157.88	17.54

The maximum area was inundated from a flood depth of greater than 5 m follow by 3 to 5 m (Figure 7). Flood at a depth of greater than 3 m is sufficient to cause a maximum damage to any households if it stays for a longer period. It is also can be seen that Amarapura township is mostly affected with an area of inundation of 85 km^2, followed by Patheingyi with 52 km^2, Pyigyitagon with 7 km^2, Aungmyae-tharzan with 6 km^2, Chanmyatharzi and Mahaaungmyae with 4 km^2, and Chanayetharzan with 1 km^2. Furthermore, the flood depths between 3 to 5 m were observed in Chanayetharzan, Patheingyi, and Amarapua while more than 5 m were seen in and around the river. The rest townships were inundated with the depth of 1 to 3 m respectively.

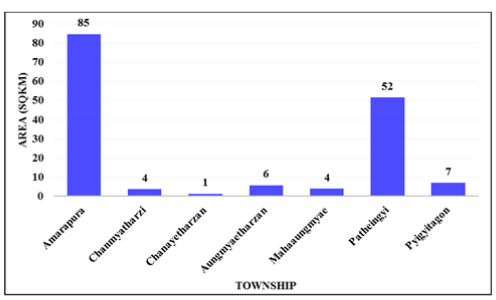

Figure 6. Flooded area in each Township.

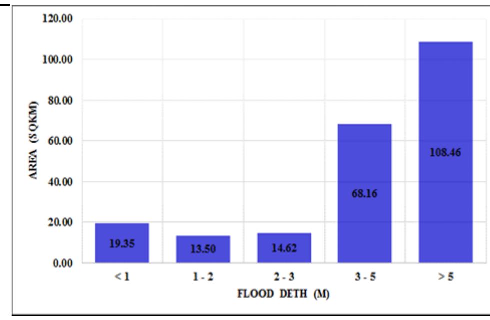

Figure 7. Depth of flooded area.

5. Conclusion

The HEC-RAS hydraulic model allowed to simulate the flood hazard mapping at the Ayeyarwady River at Mandalay city. HEC-GeoRAS environment is a useful tool as pre-processing for the visualization of the hydraulic model. Integrating flood frequency analysis, HEC-RAS, and GIS outputs allow to generate flood depth and inundated area of a given catchment. The advantage of HEC-RAS software is available to freely download at HEC-RAS website. However, the efficiency of the model using the ASTER DEM were not as good as the very high resolution for the reason of coarser resolution. Moreover, this study has limitation in accuracy assessment due to lack of field data. It is important and necessary to use field data to validate the model in order to define the accuracy of results. The model output indicated 100 years return periods flood depth varies greater than 0 to 24 m and the total inundated area is 157.88 km^2 with the maximum area under flood was 3 to 5 m in Mandalay. Amarapura is the highest affected area with an inundation of 85 km^2 followed by Patheingyi, Pyigyitagon, Aungmyaetharzan, Chan-myatharzi, Mahaaung-myae, and Chanayethar-zan township. Results from the flood hazard map will be useful in flood management, flood disaster preparedness and mitigation planning.

Acknowledgement

The authors would like to express their deepest gratitude to the Department of Meteorology and Hydrology (DMH), Myanmar for providing necessary data of the study.

Suan Sunandha Science and Technology Journal

References

Aye Ko, U. (2006). Flood Forecasting and Mitigation in Myanmar, Department of Meteorology and Hydrology, Ministry of Transport, Myanmar.

Brunner, G., & Bonner, V. (2010). HEC River Analysis System (HEC-RAS), Hydraulic Reference Manual. Version 4.1. January 2010. CA: Hydrologic Engineering Center.

Department of Meteorology and Hydrology, Ministry of Transport. (2004). DMH Annual Flood Report. Myanmar.

Department of Meteorology and Hydrology, Ministry of Transport. (2006). DMH Annual Flood Report. Myanmar.

Department of Meteorology and Hydrology, Ministry of Transport. (2010). DMH Annual Flood Report. Myanmar.

Department of Meteorology and Hydrology, Ministry of Transport. (2011). DMH Annual Flood Report. Myanmar.

Khattak, M. S., Anwar, F., Saeed, T. U. Sharif, M., Sheraz, K., & Ahmed, A. (2016). Floodplain mapping using HEC-RAS and ArcGIS: A case study of Kabul River. *Arabian Journal for Science and Engineering*, *41*(4), 1375–1390.

Sein, K. K. (2012). *Geospatial Analysis of Climate Change Impacts on Flood Frequency and Flood Risk in Mandalay.* (Master Thesis, Asian Institute of Technology).Subramanya, K. (2006). *Engineering Hydrology*, (2nd ed.). New Delhi, Tata McGraw-Hill.

Tate, E., & Maidment, D. (1999). *Floodplain mapping using HEC-RAS and ArcView GIS*. Retrieved September 10, 2015, from http://www.irfaNakar.com/gis_remote_sensing _files/HECRA-S/Floodplain Mapping Using HEC-RAS and ArcView GIS.pdf

Union of Myanmar (Department of Meteorology and Hydrology (DMH), Forest Department, Relief and Resettlement Department, Irrigation Department and Fire Services Department), Myanmar Engineering Society (MES), Myanmar Geosciences Society (MGS), Myanmar Information Management Unit (MIMU) and Asian Disaster Preparedness Center (ADPC). (2009). *Hazard profile of Myanmar*. Retrieved from http://www.preventionweb.net/files/14567_ 14567HazardReport25.8.091.pdf.

United Nations Office for the Coordination of Humanitarian Affairs (UNOCHA). (2015). *Myanmar: Floods Emergency Situation Report No.1*. Retrieved August 5, 2015 from http://www.unocha.org.

Available online at http://www.ssstj.sci.ssru.ac.th

Suan Sunandha Science and Technology Journal

Guidelines for Vehicle Robbery Prevention using Remote Blocking Signals

Narong Sangwaranatee[1*], Teerat Klangkanasub[2], Narong Kulnides[2]

[1]Department of Applied Physics, Faculty of Science and Technology, Suan Sunandha Rajabhat University,
[2]Department of Forensic Science, Faculty of Science and Technology, Suan Sunandha Rajabhat University,
U-thong Nok Road, Dusit, Bangkok 10300, Thailand
Corresponding author E-mail: *Narong.sa@ssru.ac.th

Abstract: In this paper, the radio signal remote sensing device was used to control the vehicle door switching control, which was the field trials experiment. The switching "On" and "Off" of the switching signals were used to control the vehicle door and investigated. In application, the blocking signal from the commit the remote vehicle crime in the venerable place can be protected. The results obtained have shown that the signal blocking by using another remote control over 5 meters, 10 meters and 15 meters could be achieved. The proposed models and tested results have shown that the Vehicle Brand A Model No. 1 could be blocked by 83.33 percent, while Brand A Model No.2 by 83.33 percent, Brand B Model No.1 by 40 percent, Brand B Model No.2 by 60 percent, Brand C Model No. 1 by 83.33 percent, Brand C Model No. 2 by 83.33 percent, meanwhile, the remote control for general vehicle are used radio waves with frequency 315 and 433 MHz, where the criminal will use the interference signals to form the blocking (jamming) signals, the vehicle can be robbed.

Keywords: Vehicle robbery prevention, Remote sensing, Remote control, Radio signal transmission.

1. Introduction

Security is one of the most factors that is needed in all societies, where the crimes can be prevented and the societies secure. One of the items that are required to prevent and be secure is the vehicle (car), which is actually parked within the parking places. The vehicle robbery has been the important problem of world society, which is required the key issue to solve and manage, which are many concern techniques reported, for instance, closed circuit television (CCTV) (Wilson., 2005), security person and service, global positioning system (GPS) and general packet radio service (GPRS) (Satyanarayana et al., 2013) tracking systems and Ad hoc networks (Zhou et al., 1999), etc. Although, there are many techniques available today, the committed crime of cars is still increased, especially, in the parking place that assumes to be the best secure place. Thus, the searching of the reliable techniques that can be applied efficiently and cost effectively is needed. In this work, we have proposed and investigated the simple technique that can be used for vehicle robbery prevention by the remote blocking signal, where the other radio signals from the different sources can be blocked and not access the active vehicle remote control, therefore, the committed crime cannot be done. The operation system was formed and tested by a simple arrangement, where the field trials and tests were investigated and data recorded, from which the results obtained have shown that such a proposed system can be used to prevent the vehicle commit crime, especially, in the certain area, for example, within the 15 meter range in the parking area, in which the interference signals can be blocked and the vehicle secure. Where more details are given in the following sections.

2. Operating System

In the case of blocking signals is applied to commit the crime, where the criminals often aim for spacious parking lots in the public places, for example, department stores and public streets, where they are not very common car access functions, which are the immobilizer and the remote keyless entry system. For more advanced systems passive entry and passive start, functions are implemented that allow unlocking or starting of the car by simply getting close to it. Figure 1 shows the remote blocking signal prevention system using the radio frequency (RF) signal transmission basis. The TI RFID (radio frequency identification and detection) automotive products offer market unique features and performance. All car side products are optimized for full integration into the Central Body Control Module (BCM). The Immobilizer LF (low

Suan Sunandha Science and Technology Journal

pass filter) antenna could be easily connected to the LF base station with a flexible cable length up to 13 feet (4 m). The cable length could be varied without

changing the adaptation to the base station. The integration of the base station reduces system component count and space requirements.

The Controller Entry Device manages the Immobilizer communication and pushes button interaction. During sleep state the devices enters a special low power mode with only 60nA current consumption. By pressing a push button the device wakes up and controls an external UHF (ultra-high frequency) transmitter or transceiver. Security keys and rolling codes could be stored in the integrated EEPROM memory. This memory is accessible over the LF interface without support from the battery in the key fob. The Controller Entry Device offers a special battery charge mode; to achieve faster charging it's recommended to add a charging amplifier device on the base station side. The external resonant circuit with an LF coil and a resonant capacitor could be trimmed to the correct resonant frequency with the integrated trimming capability achieving an easy way to eliminate part tolerances.

The pin-to-pin and software compatible devices are available offering an easy way of scalability from standard one-way communication to high-end bi-directional communication. The UHF device family comes with an easy to use SPI interface where all parameters of a UHF link could be configured. All building blocks of a UHF system are integrated into the devices requiring only one external oscillator, a matching network and the UHF antenna itself. The receiver and transceiver come with an integrated polling mode (wake on radio).

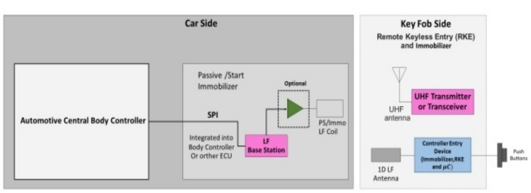

Figure 1. Schematic diagram of a remote blocking system prevention

The power supply is connected to the 12V or 24V board net and regulates down/up to voltages for DSP (digital signal processing), µC, memory and ICs (integrated circuits) and functions DVD drive, communication interfaces, display biasing and backlighting. The need for many different power rails makes the design of the power supply a critical task when trying to design for size, cost, and efficiency. Linear regulators with low quiescent current help reduce battery leakage current during standby operating modes (ignition off), are load dump voltage tolerant for directly battery connected devices, and need low drop out and tracking for low

battery crank operation. Beyond providing increased conversion efficiencies, switching power supplies provide electromagnetic immune (EMI) improve- ment with slew rate control of the switching FET(field effect transistor), Frequency hopping, spread spectrum or triangulation method for attenuation of peak spectral energy, Low current (Iq), soft start for power sequencing and inrush current limitation, Phased switching for multiple SMPS's regulators to minimize input ripple current and lower input capacitance, higher switching frequency for smaller components (L and C's), and SVS functions for brown out indications.

The allowed data exchange between independent electronic modules in the car as well as the remote sub-modules of the BCM and RFID system. High-Speed CAN (up to 1Mbps, ISO 119898) is a two wire, fault tolerant differential bus. With a wide input common mode range and differential signal technology, it serves as the main vehicle bus type for connecting the various electronic modules in the car with each other. LIN supports low speed (up to 20 kbps) single bus wire networks, primarily used to communicate with remote sub-functions of the BCM system.

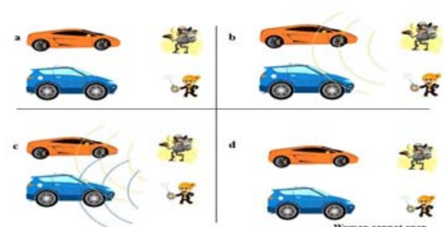

Figure 2. The blocking signals that use to commit the remote vehicle crimes

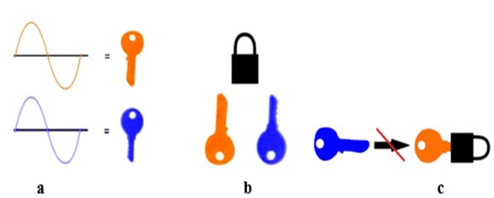

Figure 3. The blocking signal details

Figure 2, the criminal stands by and waits for the victim to bring a car to parking radius that can be blocked by the remote signal (Figure 2a). The criminal presses the remote control to send a signal

Suan Sunandha Science and Technology Journal

to the car before the victim presses the remote control to lock the car (Figure 2b). The second signal is jammed (interfered) (Figure 2c). The victim cannot open and close the doors herself (Figure1d). When the victim is leaving the car, she presses the remote control to lock the car, which can be seen that

the two signals of the car are now jamming. So, the victim is not able to both lock and unlock the car. The first signal was already jamming as shown in (Figure 2d). Even though remote virtual keys are in the same size, the size of each tooth is different (Figure 3a).The car is like a lock, so both keys can be plugged into a lock. But there is only one key that can be unlocked (Figure 3 b) as a key inserted into a compatible across key (Figure 3c). From Jamming Remote, we will explain this principle simply by metaphor with key and lock; the key with the tooth as a signal, the key without tooth as a wiretapping signal and the lock as a car. Firstly access, the criminal has inserted the key, without the tooth, in the lock. So the victim cannot use his key. In this process we cannot see in our owned eyes because it is a wave, in the same way, the toothless key from criminal are not proper for the lock because it is not a type of key which can be unlocked. We will be unlocked when we using the right one, key with a tooth. But we cannot do like that causes the other key are already inserted in the keyhole. (Figure 3c).From testing by using the sample car, we try to press the lock button on the remote control which is not matching with this car and holds this button in different area 5, 10, and 15 meters for a tapping remote control signal, from which the experiment was observed and data recorded, from which the testing distance used is as shown in Figure 4.

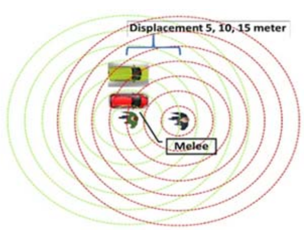

Figure 4. The remote blocking and tapping signals from the vehicles over 5 m 10 m and 15 m.

3. Experiments and Results

From experimental results, as shown in Table 1, in order to detect the blocking signals with a wiretap from remote vehicles over 5 meters, 10 meters, and 15 meters, it was found that the experiment Brand A Model 1 can be blocked 83.33 percent, where Brand A Model 2 can be blocked 83.33 percent. Brand B Model 1 can be blocked by 50 percent, where Brand B Model 2 can be blocked by 50 percent. Brand C Model 1 can be blocked by 83.33 percent, where Brand C Model 2 can be blocked by 83.33 percent. From assumption between car models and signal disturbance, their relationship was assign as follows. H0: Disturbance signal has effect to car model (Priority $\alpha = 0.05$), H1: Disturbance signal has not

effect to car model (Priority $\alpha = 0.05$). In Table 2, the result shown Pearson Chi-Square = 6.0, df = 5, Sig = 0.306. This means car A Model 1 related to the remote controls. The disturbance signal> α (0.05) $\rightarrow$ sig, which reject the null hypothesisH1 (bolt parameters are related). In Table 3, the result shown Pearson Chi-Square = 6.0, df = 5, Sig = 0.306. This means car A Model 2 related to the remote controls. The disturbance signal >α (0.05) $\rightarrow$ sig, which reject the null hypothesis H1 (bolt parameters are related). In Table 4, the result shown Pearson Chi-Square = 6.0, df = 5, Sig = 0.306. This means car B Model 1 related to the remote controls. The disturbance signal >α (0.05) $\rightarrow$ sig, which reject the null hypothesisH1 (bolt parameters are related). In Table 5, the result shown Pearson Chi-Square = 6.0, df= 5, Sig = 0.306. This means car B Model 2 related to the remote controls. The disturbance signal >α (0.05) $\rightarrow$ sig, which reject the null hypothesisH1 (bolt parameters are related). In Table 6, the result shown Pearson Chi-Square = 6.0, df = 5, Sig = 0.306. This means car C Model 1 related to the remote controls. The disturbance signal >α (0.05) $\rightarrow$ sig, which reject the null hypothesisH1 (bolt parameters are related). In Table 7, the result shown Pearson Chi-Square = 6.0, df = 5, Sig = 0.306. This means car C Model 2 related to the remote controls. The disturbance signal >α (0.05) $\rightarrow$ sig, which reject the null hypothesisH1 (bolt parameters are related).

4. Conclusion

We have reported the investigations of vehicle crime prevention using the remote blocking signal prevention. From the experiment of blocking signal of the remote control with radio wave tapping, the various different results were obtained. The vehicle remote control device used was obtained from the factory, with 315 and 433 MHz frequencies. The working process of each car was performed by the same situation. In which the signal from source was transmitted to the receiver attached in the car for lock / unlock program, which was found that that the signal was blocked by the jamming signals because the remote control signal on the same wavelength was interfered and cancelled. Moreover, the tapping signal of each remote

Suan Sunandha Science and Technology Journal

control signal is different because the signal is not matched, in which the tapping signal is not working and caused the signals with different frequencies have different wavelengths and amplitudes.

Table 1. Interference of the remote control of the car Brand A, B, and C.

The remote control of cars for blocking signal		Brand A A1	A2	Brand B B1	B2	Brand C C1	C2
Brand A	A1	✓	✓	×	×	✓	✓
	A2	✓	✓	×	×	✓	✓
Brand B	B1	✓	✓	✓	✓	✓	×
	B2	✓	✓	✓	✓	✓	✓
Brand C	C1	✓	✓	×	×	✓	✓
	C2	×	×	✓	✓	×	✓
Total		5	5	3	3	5	5

Table 2. Results of Chi–Square Tests car A model 1

	Value	df	Asymp.Sig (2 sided)
Pearson Chi-Square	6.000[a]	5	.306
Likelihood Ratio	5.407	5	.368
Linear – by – Linear Association	2.143	1	.143
N of Valid Cases	6		

Table 3. Results of Chi–Square Tests car A model 2

	Value	df	Asymp.Sig (2 sided)
Pearson Chi-Square	6.000[a]	5	.306
Likelihood Ratio	5.407	5	.368
Linear – by – Linear Association	2.143	1	.143
N of Valid Cases	6		

Table 4. Results of Chi–Square Tests car B model 1

	Value	df	Asymp.Sig (2 sided)
Pearson Chi-Square	6.000[a]	5	.306
Likelihood Ratio	8.318	5	.140
Linear – by – Linear Association	1.190	1	.275
N of Valid Cases	6		

Table 5. Results of Chi–Square Tests car B model 2

	Value	df	Asymp.Sig (2 sided)
Pearson Chi-Square	6.000[a]	5	.306
Likelihood Ratio	8.318	5	.140
Linear – by – Linear Association	1.190	1	.275
N of Valid Cases	6		

Table 6. Results of Chi–Square Tests car C model 1

	Value	df	Asymp.Sig (2 sided)
Pearson Chi-Square	6.000[a]	5	.306
Likelihood Ratio	5.407	5	.368
Linear – by – Linear Association	2.143	1	.143
N of Valid Cases	6		

Table 7. Results of Chi–Square Tests car C model 2

	Value	df	Asymp.Sig (2 sided)
Pearson Chi-Square	6.000[a]	5	.306
Likelihood Ratio	5.407	5	.368
Linear – by – Linear Association	.086	1	.770
N of Valid Cases	6		

References

Wilson, D. (2005). Behind the cameras: monitoring and open-street CCTV surveillance in Australia, *Security Journal*, *18*, 43-54, doi:10.1057/palgra-ve.sj.8340190.

Satyanarayana, K., Sarma, A. D., Sravan, J., Malini, M., & Venkateswarlu, G. (2013). GPS and GPRS based telemonitoring system for emergency patient transportation, *Journal of medical Engineering, 13*,1-9, doi:10.1155/2013/ 363508

Zhou, L., & Haas, Z. J. (1999). Securing Ad Hoc Networks, *IEEE Networks*, *13*,24-30, doi:10.1109/65.806983.

Alchekh Yasin, S.Y., Yrfanean, A.R., Mosavi, M.R., & Mohammadi, A. (2014). An effective approach for simulating the two-color infrared seekers, *Infrared Physics & Technology, 67*,73–83, doi: 10.1016/j.infrared.2014.05. 004.

Suan Sunandha Science and Technology Journal

Ishibashi, Y., & Fukui, M. (2012) Mechanism of the jamming transition in the two-dimensional traffic networks, *Physica A: Statistical Mechani-cs and its Applications, 391*, 6060-6065, doi: 10.1016/j.physa.2012.06.049.

Xiaoqi, L., Baohua, Z., Ying, Z., He, L., & Haiquan, P. (2014).The infrared and visible image fusion algorithm based on target separation and sparse representation, *Infrared Physics & Technology, 67*,397-407, doi:10.1016/j.infrared.2014.09.007.

Olmos, P. M., & Murillo-Fuentes, J. J. (2012). Remote detection of a frequency jammer operating in the down link of a cellular system, *Wireless Personnel Communication*, *63*, 861–870, doi:10.1007/s11277-010-0171-9.

SSSTJ

www.ssstj.sci.ssru.ac.th

www.ssstj.sci.ssru.ac.th

www.facebook.com/SSSTJ.Journal

Faculty of Science and Technology, Suan Sunandha Rajabhat University
1 U-thong Nok Road , Dusit, Bangkok ,Thailand 10300
Tel : (+66)2 160 1040 - 45 Fax : (+66)2 160 1046